AD-A133 123 ALGAASSB VAPOR PHASE EPITAXY AND LASER PROGRAM(U) 1/2
ROCKWELL INTERNATIONAL THOUSAND OAKS CA
MICROELECTRONICS RESE.. R CHIN JUN 83 MRDC41078.9FR
UNCLASSIFIED RADC-TR-83-127 F19628-80-C-0130 F/G 20/12 NL

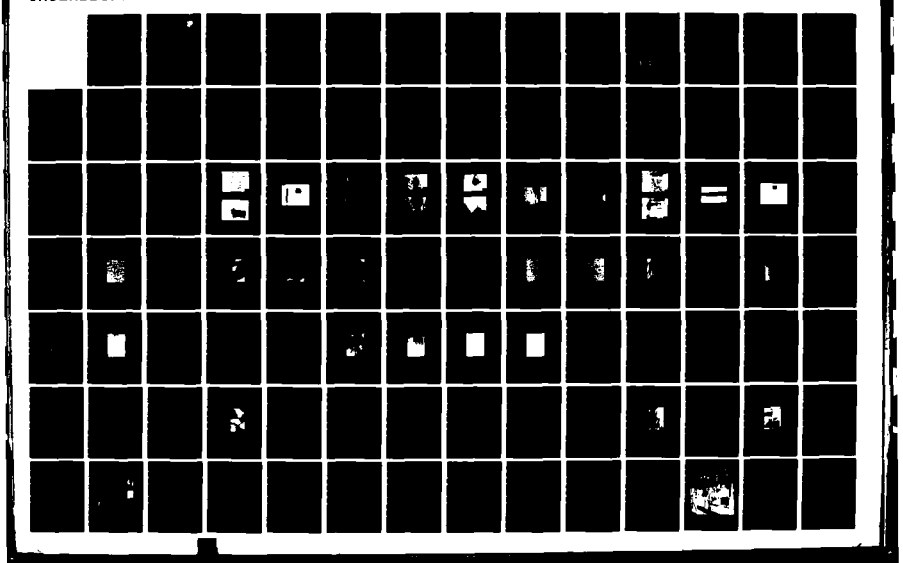

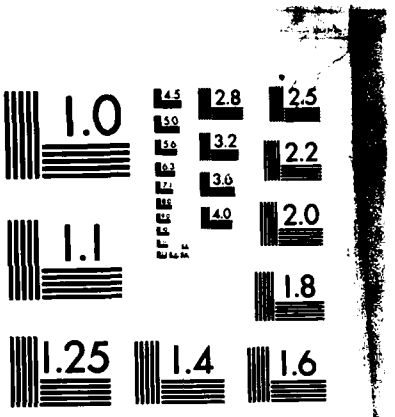

MICROCOPY RESOLUTION TEST CHART
NATIONAL BUREAU OF STANDARDS-1963-A

(12)

RADC-TR-83-127
Final Technical Report
JUNE 1983

AlGaAsSb VAPOR PHASE EPITAXY AND LASER PROGRAM

Rockwell International

R. Chin

APPROVED FOR PUBLIC RELEASE; DISTRIBUTION UNLIMITED

ROME AIR DEVELOPMENT CENTER
Air Force Systems Command
Griffiss Air Force Base, NY 13441

This report has been reviewed by the RADC Public Affairs Office (PA) and is releasable to the National Technical Information Service (NTIS). At NTIS it will be releasable to the general public, including foreign nations.

RADC-TR-83-127 has been reviewed and is approved for publication.

APPROVED: D Eirug Davies

D. EIRUG DAVIES
Project Engineer

APPROVED: Harold Roth

HAROLD ROTH, Director
Solid State Sciences Division

FOR THE COMMANDER: John P. Huss

JOHN P. HUSS
Acting Chief, Plans Office

If your address has changed or if you wish to be removed from the RADC mailing list, or if the addressee is no longer employed by your organization, please notify RADC (ESO), Hanscom AFB MA 01731. This will assist us in maintaining a current mailing list.

Do not return copies of this report unless contractual obligations or notices on a specific document requires that it be returned.

UNCLASSIFIED

SECURITY CLASSIFICATION OF THIS PAGE (When Data Entered)

REPORT DOCUMENTATION PAGE		READ INSTRUCTIONS BEFORE COMPLETING FORM
1. REPORT NUMBER RADC-TR-83-127	2. GOVT ACCESSION NO.	3. RECIPIENT'S CATALOG NUMBER
4. TITLE (and Subtitle) AlGaAsSb VAPOR PHASE EPITAXY AND LASER PROGRAM		5. TYPE OF REPORT & PERIOD COVERED Final Technical Report OCT. 80 - OCT. 82 6. PERFORMING ORG. REPORT NUMBER MRDC41078.9FR
7. AUTHOR(s) R. Chin		8. CONTRACT OR GRANT NUMBER(s) F19628-80-C-0130
9. PERFORMING ORGANIZATION NAME AND ADDRESS Rockwell International 1049 Camino Dos Rios Thousand Oaks CA 91360		10. PROGRAM ELEMENT, PROJECT, TASK AREA & WORK UNIT NUMBERS 62702F 46001741
11. CONTROLLING OFFICE NAME AND ADDRESS Rome Air Development Center (ESO) Hanscom AFB MA 01731		12. REPORT DATE June 1983 13. NUMBER OF PAGES 106
14. MONITORING AGENCY NAME & ADDRESS(if different from Controlling Office) Same		15. SECURITY CLASS. (of this report) UNCLASSIFIED 15a. DECLASSIFICATION/DOWNGRADING SCHEDULE N/A

16. DISTRIBUTION STATEMENT (of this Report)

Approved for public release; distribution unlimited

17. DISTRIBUTION STATEMENT (of the abstract entered in Block 20, if different from Report)

Same

18. SUPPLEMENTARY NOTES

RADC Project Engineer: D. Eirug Davies (ESO)

19. KEY WORDS (Continue on reverse side if necessary and identify by block number)

State-of-the-art silica-based optical fibers
III-V quarternary materials systems
metalorganic chemical vapor deposition (MOCVD)
Schottky barrier photodiodes
gas phase stoichiometry
metal alkyl injection sequence
epitaxial crystal growth

20. ABSTRACT (Continue on reverse side if necessary and identify by block number)

As the transmission of glass optical fibers has been reduced to near the theoretical limits in the 1.2-1.6 μm wavelength range, the interest in optical emitters and detectors operating in this spectral range has increased. Currently, state-of-the-art silica-based optical fibers have been produced with minimum loss of 0.2 dB/km at a wavelength of λ = 1.55 μm. The dispersion at this wavelength is also extremely low (~17 sp/nm-km). Emitters and detectors for this spectral region have been fabricated in two

DD FORM 1 JAN 73 1473 EDITION OF 1 NOV 65 IS OBSOLETE

UNCLASSIFIED

SECURITY CLASSIFICATION OF THIS PAGE (When Data Entered)

of the III-V quaternary materials systems; i.e., A[illegible]aAsSb and InGaAsP. The emphasis of this program was to develop the metalorganic chemical vapor desposition (MOCVD) materials technology for the growth of AlGaAsSb-GaSb and AlGaAsSb-InAs for heterostructure devices.

Described in this work is the successful demonstration of the hetero-epitaxy of lattice-matched GaAsSb-InAs, GaSb/InAs, GaAlSb/GaSb with AlSb mole fractions up to 0.37, and n- and p-type GaSb/GaSb structures by MOCVD. In addition, Schottky barrier photodiodes fabricated from material grown by MOCVD clearly show that high quality crystalline material can be obtained using this process.

Covered in detail for the hetero-epitaxial structures described above are the effects upon epitaxial quality of substrate orientation, growth temperature, gas phase stoichiometry, use of TMGa vs TEGa, overpressure of Column V species, substrate cleaning, and doping by using H_2Se. With these parameters under control, high quality hetero-epitaxy is shown to be readily obtained using the MOCVD process.

TABLE OF CONTENTS

LIST OF FIGURES

LIST OF FIGURES

LIST OF FIGURES

LIST OF TABLES

FOREWORD

This report was prepared by the Rockwell International Microelectronics Research and Development Center under Contract No. F19628-80-C-0130. This work covers the period October, 1980 to October, 1982.

The Principal Investigator for the project was Raymond Chin. The principal support in this work was provided by K. L. Hess. The program manager was P. D. Dapkus. The program manager for this project from Rome Air Development Center, Hanscom Air Force Base was E. R. Davies.

1.0 INTRODUCTION AND SUMMARY

1.1 Introduction

As the transmission loss of glass optical fibers has been reduced to near the theoretical limits in the 1.2-1.6 μm wavelength range, the interest in injection lasers emitting in this spectral region has increased. Currently, state-of-the-art silica-based optical fibers have been produced with a minimum loss of 0.20 dB/km at a wavelength of λ = 1.55 μm.[1] The wavelength dispersion at this wavelength is also extremely low (~ 17 ps/nm-km). The injection lasers designed for use with these low loss, low dispersion fibers have been fabricated in two of the III-V quaternary materials systems,[2-4] i.e., $Al_{1-x}Ga_xAs_{1-y}Sb_y$ and $In_{1-x}Ga_xAs_{1-y}P_y$. These quaternary semiconductors are also excellent candidates for the fabrication of other important optoelectronic devices, in particular, high efficiency heterojunction solar cells with a multiple bandgap structure and high speed heterojunction phototransistors and photodiodes.

To date, most of these device structures have been grown by liquid phase epitaxy (LPE), although some work has been reported on the growth of the ternary compounds $In_{1-x}Ga_xAs$ and $Ga_xAs_{1-y}Sb_y$[5-7] by molecular beam epitaxy (MBE). Both of these materials technologies have certain inherent disadvantages for the large scale cost-effective commercial production of the optoelectronic devices mentioned above.

The emphasis of this program was the development of another materials technology, namely metalorganic chemical vapor deposition (MOCVD), for the growth of $Al_{1-x}Ga_xAs_{1-y}Sb_y$-InAs and $Al_{1-x}Ga_xAs_{1-y}Sb_y$-GaSb heterojunction alloys and devices. Scientists at Rockwell International's Microelectronics Research and Development Center (MRDC) have shown that this process is capable of growing $Al_xGa_{1-x}As$-GaAs double heterostructure (DH) lasers with very low threshold current densities, and have also demonstrated cw laser operation of MOCVD $Al_xGa_{1-x}As$-GaAs DH lasers with unique properties.[8-29] In addition, high performance heterojunction phototransistors have been grown by MOCVD.[30]

Obviously, the exention of this technology to the wavelength region of 1.0-1.6 μm would bring large scale processing and manufacturing to optical communication devices operating at that wavelength. The issue of manufacturability is a key factor of the MOCVD growth technique. The uniformity and control of thickness, doping, and lack of melt residue that is associated with LPE make MOCVD an attractive process. Large substrate sizes (e.g., > 2" O.D.) and high yield substantially reduce per unit processing costs. In addition, device designs, such as quantum-well heterostructures, are readily fabricated using this process. These benefits provide the driving force to develop technology based on MOCVD for 1.0-1.6 μm optoelectronic devices.

1.2 Summary

The major results of this program are summarized in this section. The fact that little was known prior to the start of this program about the growth of antimonide-based compounds by MOCVD made necessary substantial development work. This required that a number of parameters of the crystal growth process be studied to obtain high quality epitaxial film. These included growth temperature, gas phase stoichiometry of three gases, substrate orientation, effects of different alkyl groups, and the overpressures of the group V elements. In spite of the large number of interacting parameters, we have successfully demonstrated the growth of high quality epitaxial layers upon both InAs and GaSb substrates. Some of the achievements of this program are:

- The demonstration of GaAsSb/InAs heterostructures grown at 550°C
- The demonstration of GaSb/InAs heterostructures
- The demonstration of GaAlSb with AlSb mole fractions as high as 0.37
- The demonstration of GaAsSb/GaSb heterostructures
- The demonstration of GaSb/GaSb structures grown from 550-625°C

Double crystal x-ray data and optical microscopy showed the epitaxial layers to have narrow linewidths and specular surfaces, respectively.

Both n-type and p-type film GaSb were demonstrated in this program. Au-Schottky metal deposited on n-type Se-doped GaSb creating Schottky diodes were shown to exhibit photoresponse. This verifies that optical device quality antimonide-based materials can be fabricated using the metalorganic process.

Listed here in more detail are the findings for different epitaxial layers grown upon either GaSb or InAs substrates.

GaSb Eptaxial on GaSb Substrates

- For hillock-free epitaxial layers, it was necessary to grow upon GaSb substrates which were oriented 5° off the <100> toward the <110>.

- Trimethylgallium (TMGa) resulted in growth rates five to ten times greater than triethylgallium (TEGa).

- Deposition could be performed from growth temperatures of 550°C to 625°C with the resulting epitaxial layers having good surface morphology.

- Pre-gallium deposition during the substrate heating phase was detrimental to achieving epitaxial film growth, while a controlled pre-antimony deposition seemed to have no effect.

- Variation of the stoichiometry of the reactant vapors over an extremely wide range resulted in no change in the conductivity type of the film. Only p-type films were obtained.

- Substrate cleaning procedure was critical for specular epitaxial nucleation.

GaAlSb Epitaxy on GaSb Substrates

- Hillock-free deposition required GaSb substrates which were 5° off the <100> toward the <110>.

- $Ga_{1-x}Al_xSb$ films with AlSb mole fractions of up to 0.37 have been grown at T ≈ 620°C.

- The AlSb mole fraction is limited to $x \lesssim 0.37$ in films of $Ga_{1-x}Al_xSb$, regardless of the amount of trimethylaluminum (TMAl) in the reactor chamber when both TMAl and TMGa are present.

- X-ray rocking curves of AlSb show considerable line broadening and intensity attenuation when grown under the same conditions as $Ga_{1-x}Al_xSb$ ($x < 0.37$).

GaAsSb or GaSb Epitaxy on InAs Substrates

- Growth temperatures of 550°C or less were required to obtain specular GaAsSb/InAs wafers.

- Arsine predeposition starting at room temperature resulted in the best substrate surfaces.

- GaAsSb could be grown exactly lattice-matched to InAs.

Although light emitters were not fabricated due to time limitations, the substantial progress in the crystal grown technology clearly shows that MOCVD is a suitable means to achieve such structures.

2.0 TECHNICAL DISCUSSION

2.1 Properties, Applications & Previous Growth Studies in GaAlAsSb

The quaternary $Al_{1-x}Ga_xAs_{1-y}Sb_y$ can be thought of as a solid solution of the four binary III-V compound semiconductors, AlAs, GaAs, GaSb and AlSb. The lattice constant, a_o, and the energy gap between the valence band and the lowest conduction band minimum, E_g, is a function of the alloy composition, i.e., $a_o = a_o(x,y)$ and $E_g = E_g(x,y)$. The dependence of $a_o(x,y)$ and $E_g(x,y)$ upon alloy composition for $Al_{1-x}Ga_xAs_{1-y}Sb_y$ is shown in Fig. 1. These results are calculated from data obtained on the binary compounds (corners of Fig. 1) and the corresponding ternaries (edges of Fig. 1). Since there are few actually measured data points for this quaternary system, the results of these calculations may be subject to error. In fact, there are significant differences between the calculated results shown in Fig. 1 and published data.

An interesting feature of Fig. 1 is that the lines of fixed lattice constant (dashed lines) are nearly normal to the lines of fixed bandgap energy (solid lines). This means that, for a given lattice constant (or substrate material), the energy gap of the lattice-matched quaternary $Al_{1-x}Ga_xAs_{1-y}Sb_y$ can be varied over a wide range, i.e., for a given value of $a_o(x,y)$, there is a wide range of corresponding values of $E_g(x,y)$. Thus, lattice-matched heterojunctions in the $Al_{1-x}Ga_xAs_{1-y}Sb_y$ quaternary system can be grown quite readily.

It is also apparent from Fig. 1 that there is a significant alloy composition regime where the lowest lying conduction band minima are indirect L minima (shaded portion of Fig. 1). While this range of $Al_{1-x}Ga_xAs_{1-y}Sb_y$ alloys would thus not be useful as the active region of DH lasers, films with these compositions could be useful as confining layers. The range of direct bandgap energies of $Al_{1-x}Ga_xAs_{1-y}Sb_y$ alloys varies from $E_g \sim 0.70$ eV (λ = 1.77 μm) to $E_g \sim 2.0$ eV (λ = 0.620 μm).

Another interesting feature of the $Al_{1-x}Ga_xAs_{1-y}Sb_y$ quaternary that is shown in Fig. 1 is that there are four readily available III-V binary

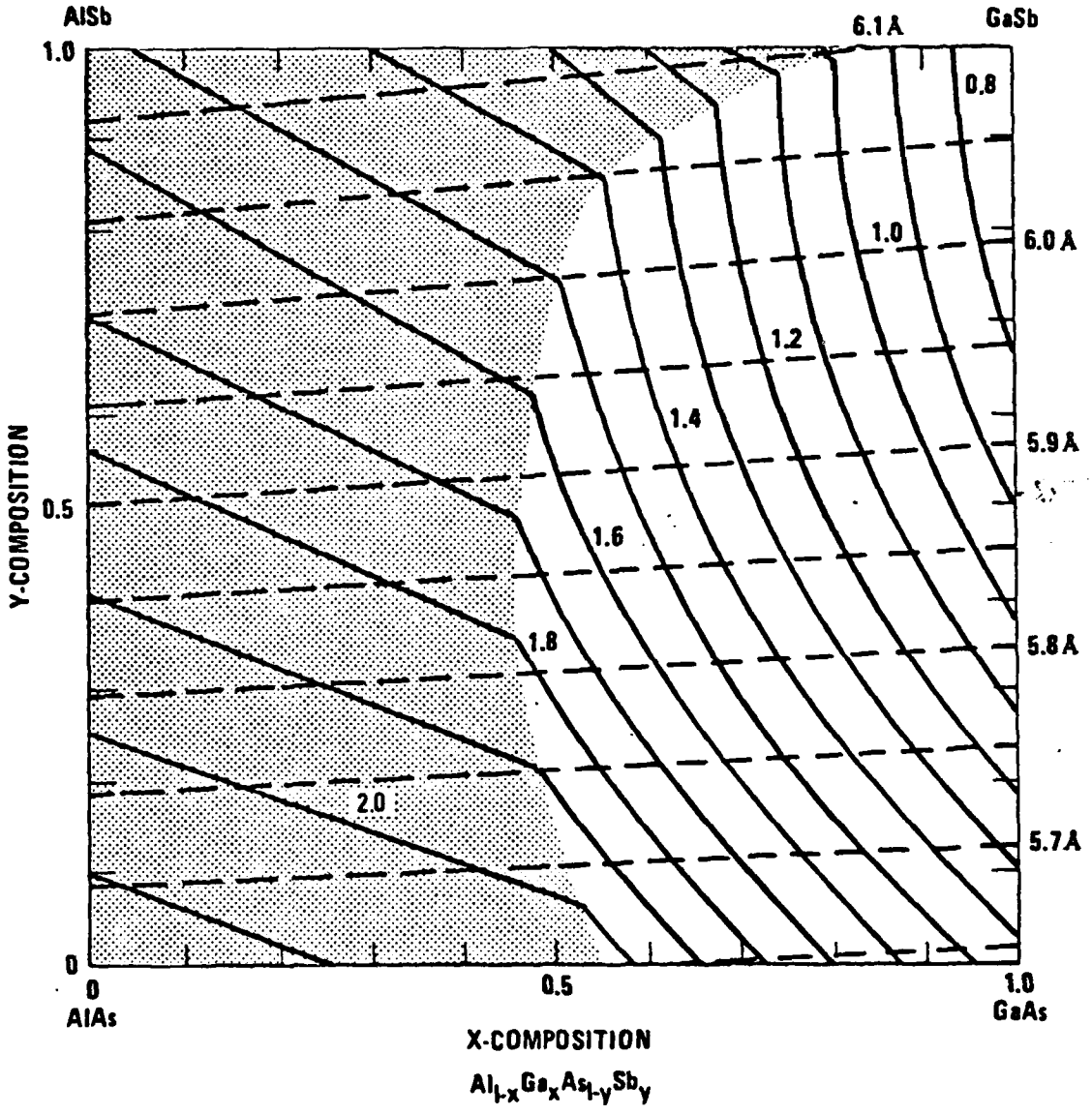

Fig. 1 $a_o(x, y)$ and $E_g(x, y)$ for $Al_{1-x}Ga_xAs_{1-y}Sb_y$.

semiconductor substrates that are potentially useful for the MOCVD growth of lattice-matched thin films, namely GaAs (a_0 = 5.654Å), GaSb (a_0 = 6.095Å), InAs (a_0 = 6.058Å) and InP (a_0 = 5.869Å). This permits the growth of a wide variety of useful $Al_{1-x}Ga_xAs_{1-y}Sb_y$ alloys. In fact, alloys throughout the total range of direct bandgaps can be grown lattice-matched (or nearly so) to one or more of these substrates. Specifically, epitaxial layers having $0.7 < E_g \lesssim 1.1$ eV can be grown on GaSb substrates; films with $0.9 < E_g \lesssim 1.7$ eV can be deposited on InP substrates; GaAs can be used as a substrate for quaternary alloys having $1.4 < E_g \lesssim 2.0$ eV; and InAs can be used as a substrate to grow alloy films with $0.74 < E_g \lesssim 1.33$ eV. It should also be possible to grow epitaxial ternary $GaAs_{1-y}Sb_y$ films that can subsequently be used as a "thin film substrate" to grow lattice-matched quaternary films with other composition ranges. As discussed below, the MOCVD process can be used to grow linearly-graded or step-graded ternary film structures to fulfill the role of a substrate. One of the objectives of the program, however, was to determine the feasibility of low threshold lasers suitable for operation at 1.55 μm or 1.3 μm (Appendix I). As a result, the GaSb or InAs substrates appeared most suitable for these two ranges. Also, InP could be employed as a substrate.

The principal electro-optic applications of $Al_{1-x}Ga_xAs_{1-y}Sb_y$ heterojunction devices are for double heterostructure injection lasers, heterostructure photodetectors, and high efficiency multiple bandgap solar cells. Other potential applications include passive optical waveguides and optical switches and modulators for monolithic integrated optical circuits. A brief description of the previously obtained results will be given below, as well as a description of previous work on the epitaxial growth of $Al_{1-x}Ga_xAs_{1-y}Sb_y$ and related materials.

Nearly all studies of the growth of $Al_{1-x}Ga_xAs_{1-y}Sb_y$ and related III-V ternary and binary semiconductors have been devoted to the growth of thin films by LPE.[31,32] The devices fabricated include high-speed $Al_{1-x}Ga_xSb$ photodetectors,[33] high efficiency LEDs,[31] and $Al_{1-x}Ga_xAsSb/Al_{1-x}Ga_xAs_{1-y}Sb_y$ DH lasers emitting at ~ 1.0 μm. An interesting feature of the LPE growth of

$Ga_xAs_{1-y}Sb_y$ is that several authors have reported the existence of a miscibility gap in the composition range $0.3 < 0.61$[33] that may, in fact, extend into the quaternary $Al_{1-x}Ga_xAs_{1-y}Sb_y$. Other workers who studied the LPE growth of $Ga_xAs_{1-y}Sb_y$ report that the solidus curve for this system is a rapidly varying function of temperature, and this apparent "miscibility gap" is directly related to the difficulty of growing from equilibrium conditions for this ternary system. It is interesting to note that this effect should not occur for the MOCVD growth of $GaAs_{1-y}Sb_y$, since the alloy composition is not controlled by an equilibrium liquid-solid diagram, but is instead uniquely determined by the relative partial pressures of AsH_3 and $(CH_3)_3Sb$ in the vapor phase. This relative partial pressure is accurately controlled by the source gas flow rates. Thus, it is expected that $GaAs_{1-y}Sb_y$ alloys can be grown by MOCVD throughout the entire composition range.

Another materials technology that has been used to grow thin films of $GaAs_{1-y}Sb_y$ is (MBE). Although work in this area has been limited, the MBE growth of $GaAs_{1-y}Sb_y$ films throughout the alloy composition has been reported.[5,6] No device materials have yet been reported.

The halide vapor phase epitaxial (VPE) growth of GaSb has been reported employing Ga, SbH_3 and HCl sources. There are no reports of the preparation of $GaAs_{1-y}Sb_y$ films by this process. Furthermore, it would be difficult, if not impossible, to grow $Al_{1-x}Ga_xAs_{1-y}Sb_y$ quaternary films by this process, owing to the extreme reactivity of $AlCl_3$ and the chemistry of this process. These same problems have prevented (thus far) the preparation of homogeneous films of $Al_{1-x}Ga_xAs$ alloys by the halide VPE process.

The use of the MOCVD process for the growth of GaSb and $GaAs_{1-y}Sb_y$ was first reported by Manasevit in 1969. While epitaxial films were obtained over a limited range of $GaAs_{1-y}Sb_y$ alloy composition, the MOCVD process should offer many unique advantages for the growth of $Al_{1-x}Ga_xAs_{1-y}Sb_y$ thin films. These advantages of the MOCVD process are described more fully in later sections.

2.2 Metalorganic Chemical Vapor Deposition

The potential of the $Al_{1-x}Ga_xAs_{1-y}Sb_y$ alloy system for optoelectronic and high speed device applications, as well as the problems inherent in the growth of this alloy by other epitaxial techniques, motivates Rockwell's proposed program. We propose to utilize the MOCVD techniques for the growth of these alloys. It is strongly felt that the features of this growth technique are ideally suited to the quaternary alloy $Al_{1-x}Ga_xAs_{1-y}Sb_y$, and its development will hasten the development of this materials technology.

2.3. MOCVD Process Description

The MOCVD process that was first demonstrated in our laboratories by Manasevit differs from other epitaxial growth processes for III-V compounds, in that the Column III metals (Al, Ga) are transported in a gaseous form to the reactor from metalorganic compounds such as TMAl and TMGa. These metalorganic compounds are volatile liquids which are introduced into the reactor by bubbling a carrier gas such as ultra-pure hydrogen through them. In this manner, several problems associated with growth from a solution (LPE) can be avoided. In addition, problems associated with establishing high temperature chemical equilibrium to transport the elements, as required in the halide transport VPE processes, can also be avoided. The Column V elements in the MOCVD process are transported as gaseous hydrides such as AsH_3 and PH_3. In simplified form, the reaction may be expressed in the following way for GaAs growth:

$$(CH_3)_3Ga + AsH_3 \xrightarrow[700^0C]{H_2} GaAs + 3CH_4\uparrow \quad . \qquad (1)$$

The vapors of the metalorganic compounds are mixed with the hydride and pyrolized at a heated substrate. In principal, by the use of appropriate metalorganic compounds and hydrides in the proper partial pressure ratio, any of the III-V compounds and alloys can be grown by this process. In fact, as will be discussed later, virtually all of the III-V compounds and most of these

ternary alloys have been grown by MOCVD. The extension of the process to the quaternary $Al_{1-x}Ga_xAs_{1-y}Sb_y$ should be possible and proceed in a similar manner:

$$(CH_3)_3Al + (CH_3)_3Ga + AsH_3 + (CH_3)_3Sb \xrightarrow[700^0C]{H_2} Al_{1-x}Ga_xAs_{1-y}Sb_y + CH_4\uparrow \quad . \qquad (2)$$

There are several distinct advantages of the general MOCVD process. Because the reactants are all gaseous, it is possible to form homogeneous gas mixtures and attain uniform composition films. Furthermore, the composition is controlled by the partial pressures of the various constituents. In turn, these can be precisely controlled with electronic mass flow controllers to control gas flow rates. There is no need to maintain a temperature gradient for the transport of any species and only the substrate need be heated. In addition, the kinetic properties of the reaction are not strongly dependent on temperature, owing to the pyrolytic nature of the reaction.

Shown in Fig. 2 is a schematic diagram of a MOCVD growth system. In Appendix II is a photograph of the MOCVD reactor used for the growth of GaAlAsSb. The major difference between the GaAlAsSb system and previous GaAlAs systems is the addition of a source of trimethylantimony (TMSb). The system consists of three subsystems. First is the stainless steel gas mixing system made up of valves and tubing to control the direction, and mass flow controllers to control the rate of gas flow. Second is the source system consisting of stainless steel bubbler cylinders in appropriate temperature controlled baths for the introduction of the metalorganic compounds into the gas system and high pressure gas cylinders for the introduction of the hydrides and dopants. Finally, the reactor growth chamber itself consists of a quartz envelope and an inductively heated susceptor for the growth reactions which result in epitaxial crystal growth.

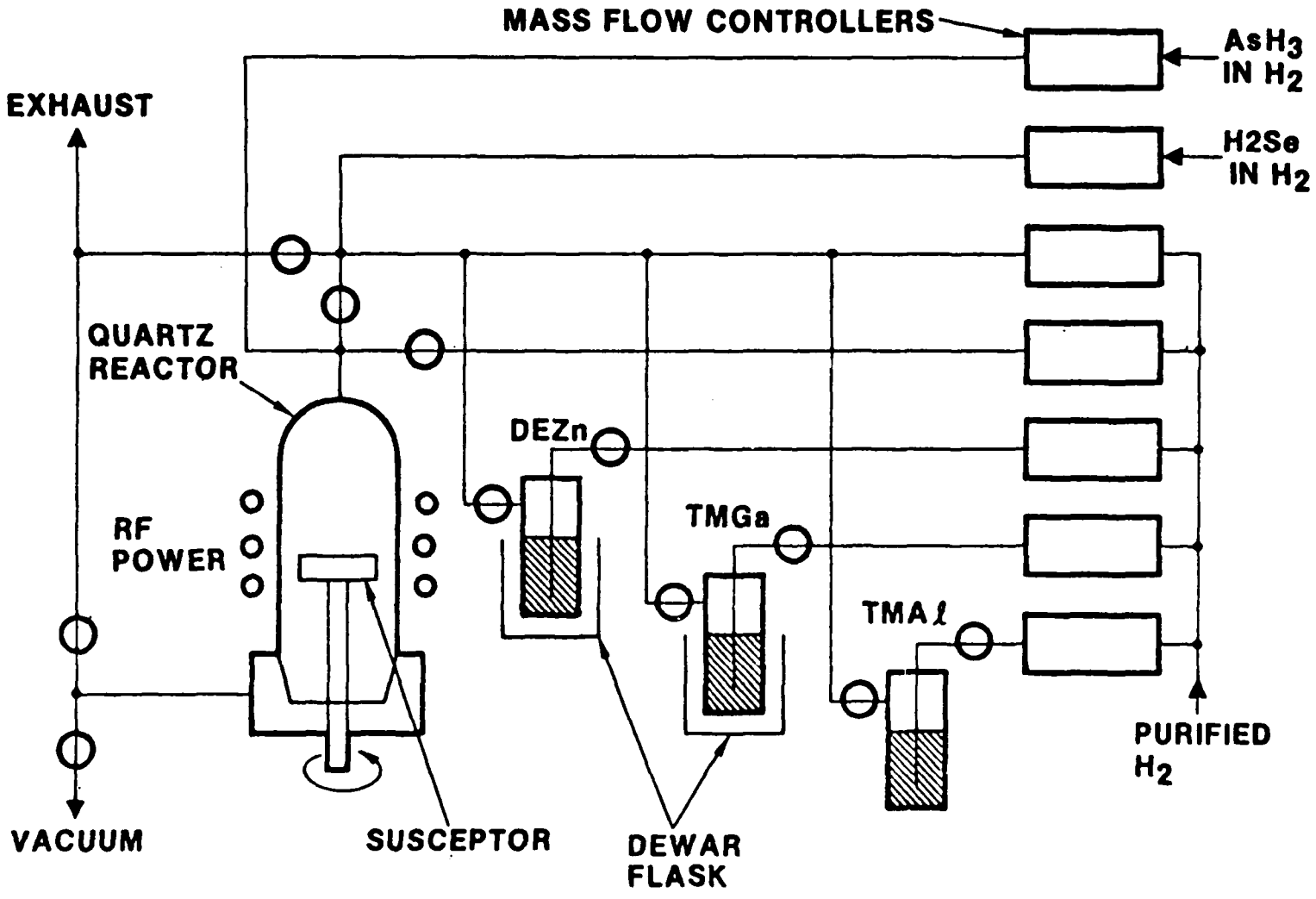

Fig. 2 Simplified reactor schematic diagram.

2.4 Advantage of the MOCVD Process

There are several important advantages which are inherent in the MOCVD process as developed by Rockwell for the growth of semiconductors.

Process Control - Only a single hot temperature zone is needed for film growth in the MOCVD process. In other processes, many of the source materials and the reaction zone are dependent upon very precisely controlled hot temperature zones regulating the vapor pressures of the reaction components and also the cooling rates during film growth. With MOCVD, the temperature of the growth process is provided by rf heating of a single susceptor on which the substrate is placed, and the walls of the reactor are essentially cool, except for the section which is very close to the susceptor and heated by radiation. Even that section is low in temperature because the growth process takes place at temperatures as low as 500-750°C.

The MOCVD growth process involves reactants which are either liquid or gaseous at room temperature. These reactants are external and upstream of the reactor and are transported by carrier gases to the reactor. The composition of the gases is easily controlled by electronic mass flow control of the species which are gaseous at room temperature and the flow of the carrier gases through the liquid species.

Multilayer Structures Can Be Easily Achieved - The changes from one materials combination to another requires merely the change of the compositions of the gas mixture. This is easily accomplished with MOCVD by exchanging one equilibrated gas mixture with another equilibrated mixture of different composition. The exchange is accomplished in a unique gas mixing system developed by Rockwell. Structures with up to 300 layers have been grown in one run in the GaAlAs/GaAs system by MOCVD.

The MOCVD Process is Scalable to High Volume - Large area, uniform surface coverage in a single growth sequence can be achieved in the same type

of commercial equipment that is used for the growth of elemental semiconductors, e.g., silicon. Thus, material costs will be reduced considerably compared with other fabrication techniques. In addition, when desirable, high growth rates compatible with product environments are achievable.

2.5 Specific Advantages of MOCVD for the Growth of $Al_{1-x}Ga_xAs_{1-y}Sb_y$

There are a number of aspects of MOCVD epitaxial growth that are of particular interest for the preparation of quaternary $Al_{1-x}Ga_xAs_{1-y}Sb_y$ epitaxial layers. By far, the single most important advantage of the MOCVD process is in the potential for accurate composition control and reproducibility. $Al_{1-x}Ga_xAs_{1-y}Sb_y$ covers a wide range of lattice constants (for direct alloys) from 5.790A-6.095A. This allows for a possible lattice mismatch, $\Delta a/a_o$, of greater than 780×10^{-4} when using GaAs as a substrate. The maximum mismatch in the AlAs/GaAs system, by comparison, is 14×10^{-4}, indicating that compositional error can be up to 56 times greater in the $Al_{1-x}Ga_xAs_{1-y}Sb_y$ system. Because of this relatively large lattice mismatch, it is essential that the alloy composition of the $Al_{1-x}Ga_xAs_{1-y}Sb$ epitaxial films be precisely controlled to prevent large amounts of strain-induced dislocations from being introduced into device structures. This degree of control can be difficult to achieve in the LPE materials technology. The MOCVD materials technology is well-suited to quaternary thin film growth, since a high degree of alloy composition control can be achieved by the precise control of source carrier gas flow rates. In addition, the MOCVD process readily permits the growth of graded bandgap structures having both linearly-graded and step-graded structures. This could be of great importance in the lattice-matched growth of III-V quaternaries that do not have the same lattice constant as readily available binary substrates.

A second advantage of the MOCVD process is the elimination of possible external contamination. For each epitaxial growth run of LPE $Al_{1-x}Ga_xAs_{1-y}Sb_y$, all solution constituents must be handled for cleaning, etching and weighing. By contrast, the source materials for MOCVD

$Al_{1-x}Ga_xAs_{1-y}Sb_y$ are maintained without interruption in a clean, contamination-free environment which is an integral part of the reactor design.

A third distinct advantage of the MOCVD process for $Al_{1-x}Ga_xAs_{1-y}Sb_y$ is that it is a simple matter to provide an As or Sb overpressure for the GaAs or GaSb substrate during the time (which is short relative to LPE processes) in which the substrate is allowed to remain at elevated temperatures near the growth temperature. This should effectively eliminate substrate surface decomposition and the need for any in-situ substrate preparation.

The MOCVD process should routinely allow accurate control and uniformity for the growth of the thin ($t < 0.2$ μm) epitaxial layers necessary for double heterostructure lasers. Such control is difficult to accomplish with LPE $Al_{1-x}Ga_xAs_{1-y}Sb_y$ epitaxial growth techniques.

The major disadvantage of MOCVD is the purity of the starting metal-organics. While this usually presents no problem for lasers and LEDs, it can drastically effect the performance of photodetector devices.

3.0 TECHNICAL APPROACH AND GOALS

3.1 Development of a MOCVD Process for the Growth of $Al_{1-x}Ga_xAs_{1-y}Sb_y$ Films Lattice-Matched to GaSb and InAs Substrates

The chemical vapor deposition process used in this program employed the metalorganic compounds TMGa, TMAl, and TMSb [or triethylantimony (TESb)] and the hydride arsine (AsH_3). This MOCVD process has already been utilized for the binary and several ternary constituents of the GaAlAsSb system, and was explored for the growth of $Al_{1-x}Ga_xAs_{1-y}Sb_y$ quaternary films throughout the alloy composition ranges that are lattice-matched to GaSb and InAs substrates. The emphasis was placed on the use of GaSb and InAs substrates, since these are available internally at Rockwell, and $Al_{1-x}Ga_xAs_{1-y}Sb_y$ alloys with the desired range of bandgap energies can be grown lattice-matched to these substrates. The major heterostructure of interest is the $Al_{1-x}Ga_xAs_{1-y}Sb_y$/InAs structure.

The principal dopant used for the growth of *n*-type films was H_2Se. This dopant source was used in all of our $Al_{1-x}Ga_xAs$-GaAs heterostructure device development.

The program approach was to first study the growth of epitaxial GaSb on GaSb substrates. Having established this baseline, the MOCVD epitaxy of GaAsSb and GaAlSb were examined. Finally, MOCVD of GaAlAsSb grown upon InAs was to be studied.

During all phases of the program, the optimal temperature of crystal growth was determined empirically by characterization of film properties. Other parameters optimized included substrate orientation, growth rate, partial pressure ratios (TMGa/TMAl) and ($TMSb/AsH_3$), gas phase stoichiometry control of Column V vapor pressures, doping level and type, and film thickness or growth rate. The optimization was performed with respect to crystalline quality, surface morphology and electrical characteristics.

The growth conditions optimal for the growth of GaSb upon GaSb substrates were not the same as those for deposition upon InAs substrates. Although this was suspected prior to the initiation of the program, the parametric changes necessary were not known. We now examine the results of this program.

4.0 GaAlAsSb EPITAXIAL FILM RESULTS BY METALORGANIC CHEMICAL VAPOR DEPOSITION

4.1 GaSb Optimization

Examined in this section are the effects of the TMGa/TEGa ratio, growth temperature, and stoichiometry ratios of III and V elements.

4.2 Substrate Types and Preparation

During the second quarter of this program, the main effort was directed toward optimizing the growth of GaSb. The growth was studied as a function of various growth parameters. The main parameters varied were the growth temperature and the mole fraction ratios of the TEGa, TMSb and H_2. In addition, various substrate materials were examined. The substrates used for epitaxial growth were:

1. GaSb n- and p-type (100)
2. GaAs undoped (111)
3. GaAs Cr doped (100)
4. InAs undoped (100)
5. Sapphire

All the substrates were organically cleaned. This process consisted of boiling the substrate in trichlorethane, acetone, and finally isopropanol for ~ 6 min (2 min/solvent). The GaSb substrates were further cleaned. First, these substrates were soaked in hydrofluoric acid for three minutes to remove any surface oxides. This was followed by a methanol rinse and a 30 second etch in 3% bromine in methanol. Finally, the substrates were rinsed in methanol and blown dry with nitrogen. After the organic cleaning, the GaAs substrates were etched in 4:1:1 H_2SO_4:H_2O:H_2O_2 and rinsed in H_2O and isopropanol. Following substrate cleaning, the general reactor operation followed is similar to that outlined in Appendix III.

4.3 Experiments and Data

The effects upon the GaSb crystalline quality of growth temperature and TEGa/TMSb flow ratios were of primary concern. TEGa was used in initial experiments because of our experience with it from previous work. In addition, it was thought that lower growth temperatures would be possible with TEGa, as compared to TMGa, owing to its lower decomposition temperature (Appendix III). A major goal was to grow epitaxial films which were free of surface features such as hillocks and metal precipitates, and which were specular in appearance; this would allow device investigations. The use of different types of substrates permitted extensive data from the samples to be collected. These are now discussed.

As mentioned earlier, growth temperatures from T = 450°C to 600°C were examined. The TEGa/TMSb ratio was optimized at a growth temperature of 550°C to produce the most specular surface (free of hillocks and defects). Using this flow ratio, the growth was also examined at 450°C, 500°C and 600°C. The particular flow rates used here are: H_2/TMSb = 13 ccpm with the bubbler temperature at 0°C; H_2/TEGa = 250 ccpm wth the bubbler temperature at 18°C; and H_2 pusher gas flow at 7 LPM. This corresponds to a molar ratio of TEGa/TMSb of 188/1. The growth time for all experiments was 50 minutes.

Since the deposited layers were p-type, the thickness of the layer was measurable only on n-type GaSb substrates or on GaAs:Cr substrates. Selected samples were examined using a scanning electron microscope apparatus. Samples grown at temperatures of 500°C, 550°C and 600°C were examined. The growth rate of GaSb on GaSb:Te varied from 200Å/min to 260Å/min and of GaSb on GaAs:Cr from 200Å/min to 240Å/min. No strong correlation between the temperature of growth and the rate of growth was observed over the temperature range studied.

For temperatures below 500°C, the epitaxial crystal layer appeared dull throughout the growth process. At a growth temperature of 500°C, the initial growth was very specular; however, as the deposition continued, the epitaxial layers became dull and hazy. This occurred for all substrates:

GaSb (undoped); GaSb (Te doped); GaAs (Cr doped); and sapphire. A SEM surface photograph of GaSb on GaSb (Te doped), taken at a magnification of 24,000, is shown in Fig. 3a. As is evident, nonuniform deposition and the appearance of droplets (metal precipitates) on the epitaxial layer result in the hazy appearance observed with the naked eye.

Figure 3b is a photograph of an EDAX analysis of GaSb (Te doped). A comparison between the substrate and the epitaxial layers showed that the deposited film had the same stoichiometry as the substrate. Shown in Fig. 3c is a photograph of a RED pattern which demonstrates that the film is a single crystal. The same type of analysis has been applied to GaSb grown on GaAs (Cr doped). The major difference between the epitaxial layer on GaAs and on GaSb is that the surface grown on GaAs exhibits a higher density of hillocks. For layers grown at 525°C and 600°C, the results were essentially the same as at 500°C.

The best epitaxial films were grown at a temperature of 550°C. At this temperature, numerous flow rate ratios of TEGa/TMSb were examined. The effect of the ratio upon crystalline quality was also examined. The molar ratio of TEGa/TMSb was varied from 49/1 to 349/1. A series of photographs (Figs. 4-8) demonstrate what happens to the surface morphology of GaSb on GaSb (Te doped) as the ratio is varied. These photographs were taken with an optical microscope using Nomarski contrast. As is evident, hillocks occur for all ratios, except when the TEGa/TMSb was equal to 188/1 (Fig. 5). The source of the hillocks was most likely due to precipitates acting as a nucleation source for off-orientation crystal growth. In order to determine if any type of surface features existed for the molar ratio (TEGa/TMSb) of 188/1, SEM microphotographs were made. Figures 9a and 9b show the surface of a GaSb at two different magnifications of 12,200 and 2,450, respectively. The small droplets which are ~ 250Å in diameter may be due to a Ga predeposition procedure employed prior to and after the growth of the GaSb. These droplets are again evident in the cross section SEM microphotographs of Fig. 10. Figure 11 shows a RED pattern taken on the sample of Fig. 5. The material is a single

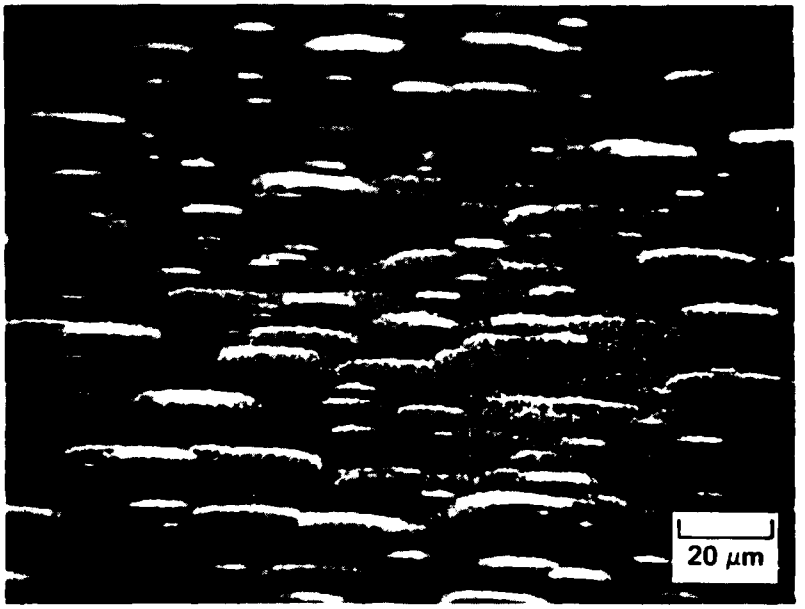

(a)

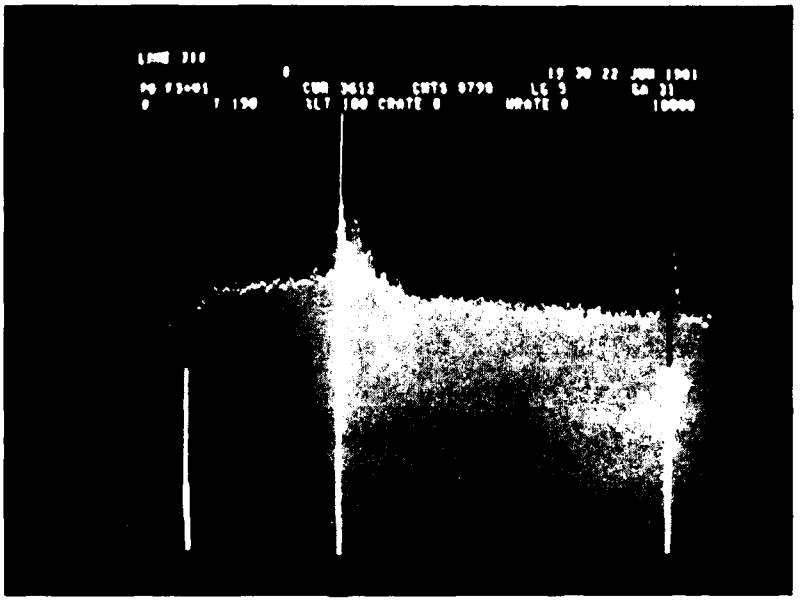

(b)

Fig. 3 a) SEM photomicrograph of a surface of GaSb grown upon GaSb,
b) EDAX analysis and RED pattern of the same wafer shown in (a).

MRDC81-14081

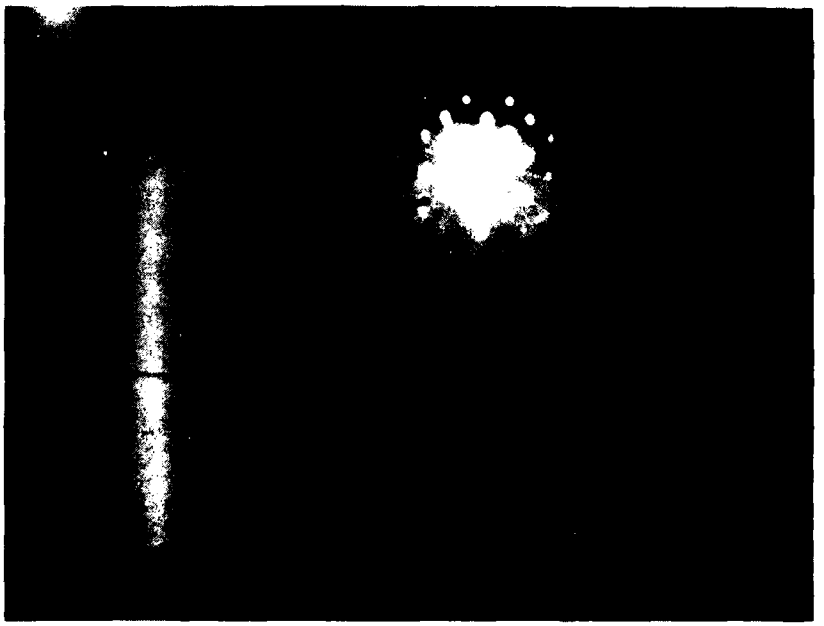

Fig. 3 (Cont.) (c) EDAX analysis and RED pattern of the same wafer shown in (a). The growth temperature used for this wafer was 500°C.

MRDC81-14076

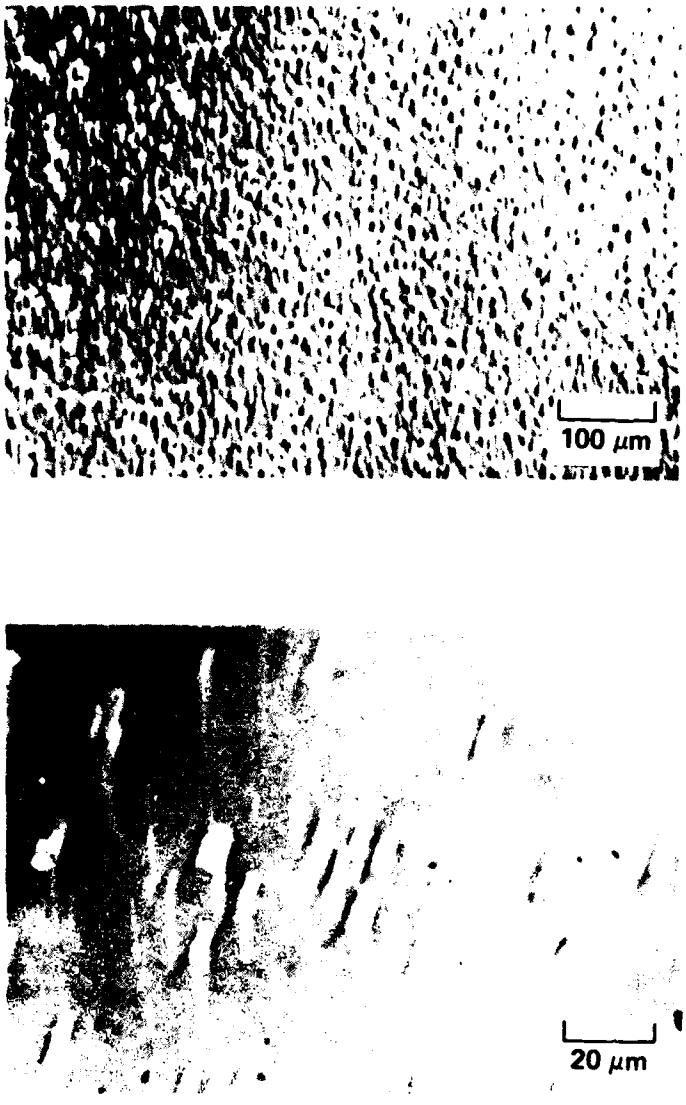

Fig. 4 a) and b) are surface photographs of GaSb grown on GaSb (Te doped) at two different magnifications. The molar flow ratio of TMGa/TMSb and growth temperature were 349/1 and 550°C, respectively.

MRDC81-14071

Fig. 5 a) and b) are surface photographs of GaSb grown on GaSb (Te doped) at two different magnifications. The molar ratio of TMGa/TMSb and growth temperature were 226/1 and 550°C, respectively.

MRDC81-14075

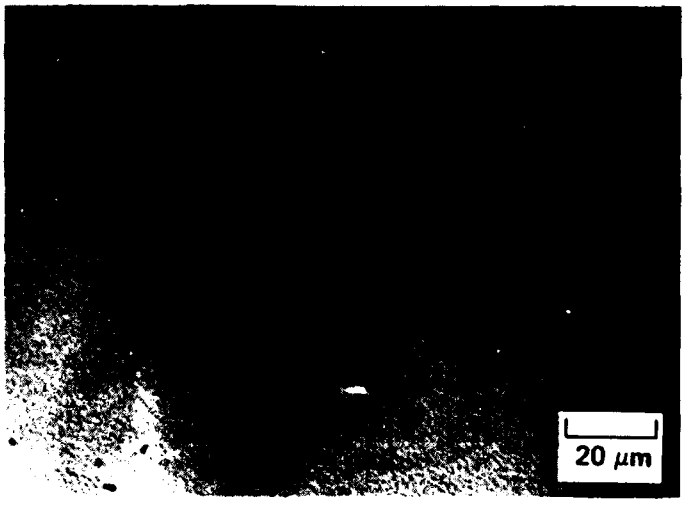

Fig. 6 a) and b) are surface photographs of GaSb grown on GaSb (Te doped) at two different magnifications. The molar ratio of TMGa/TMSb and growth temperatures were 188/1 and 550°C, respectively. b) pictures clearly the formation of hillocks.

MRDC81-14086

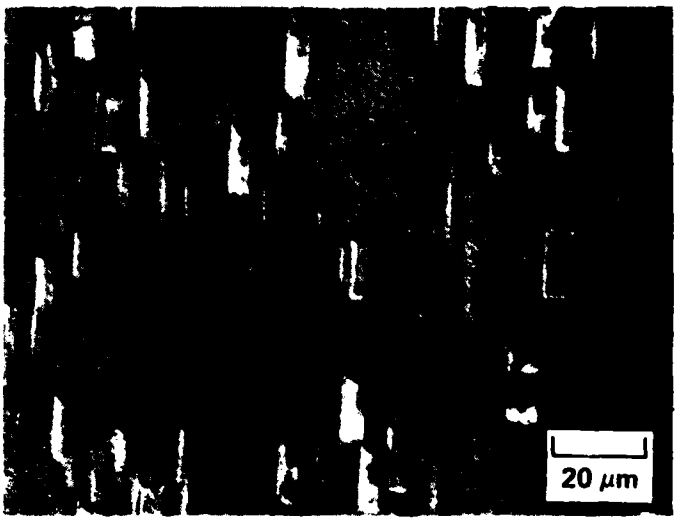

Fig. 7 Surface photographs of GaSb grown on GaSb (Te doped) at two different magnifications. The molar ratio of TMGa/TMSb and grown temperature are 98/1 and 500°C, respectively.

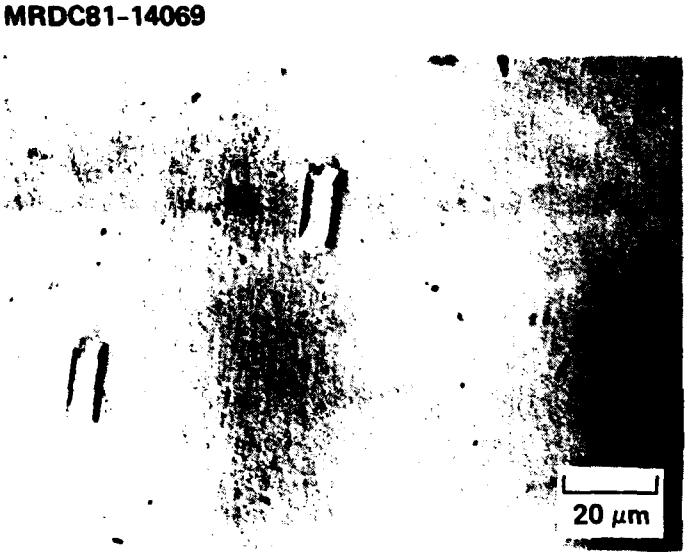

Fig. 8 Surface photographs of GaSb grown on GaSb (Te doped) at two different magnifications. The molar ratio of TMGa/TMSb and growth temperature are 49/1 and 550°C, respectively.

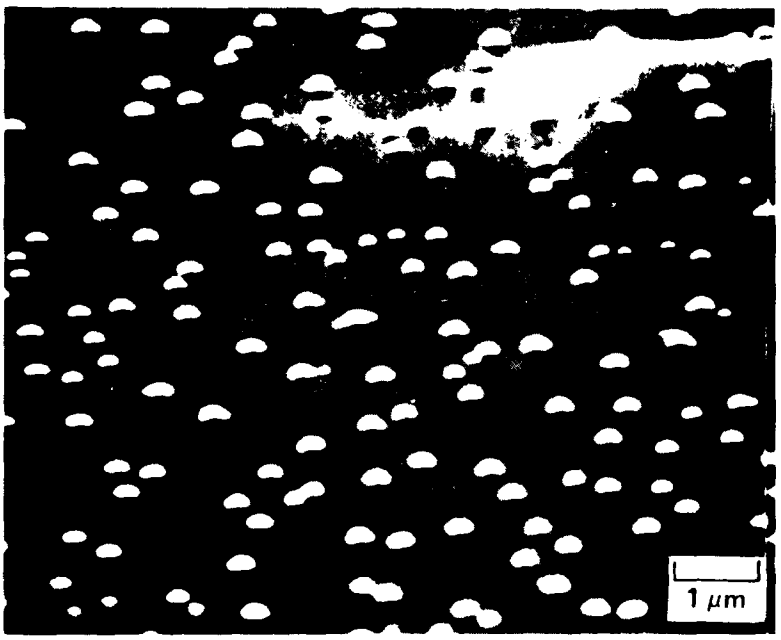

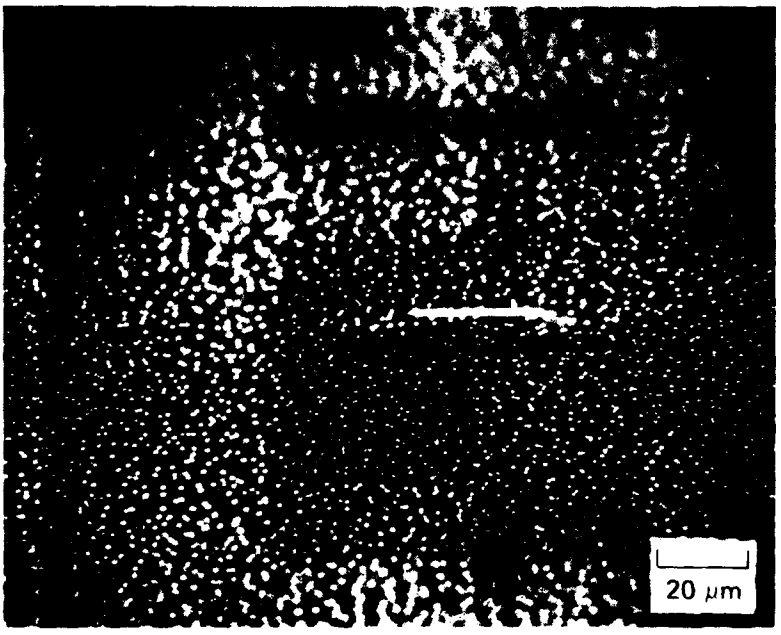

Fig. 9 SEM photomicrograph of the sample shown in Fig. 6 at two different magnifications.

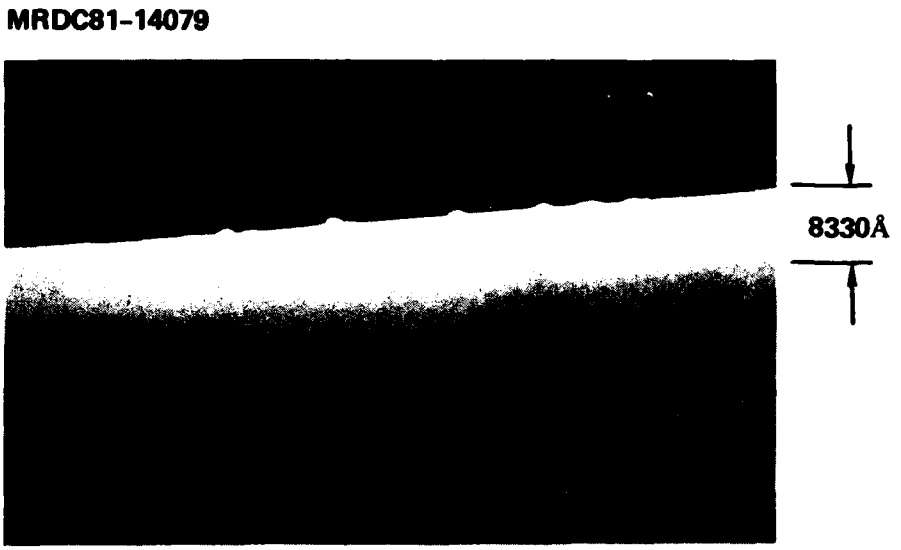

Fig. 10 SEM photomicrograph of a cross section of the sample shown in Fig. 6. From the thickness indicated, the growth rate was approximately 0.02 μm/min.

MRDC81-14083

Fig. 11 RED pattern of the GaSb sample of Fig. 6.

crystal. No samples from this group were submitted to SEM analysis for growth rate determination.

The highest quality films obtained in this set of experiments were grown at a temperature of 550°C. The optimum molar ratio at this temperature of TEGa/TMSb was approximately 188/1. Under these conditions, the films grown were the best obtained for each type of substrate.

The growth rates for these films were in the range of 0.022-0.030 μm/min. Relative to the growth rate for GaAs grown at 750°C, this is lower by approximately a factor of three. Although this rate is not intrinsically low, higher growth rates are desirable to reduce the total growth time necessary for any devices. All the films grown were p-type. No intentional doping was attempted at this early state of the material development.

For GaSb using TEGa, it has been found that the highest quality films were obtained at a growth temperature of 550°C wth a molar ratio of TEGa/TMSb ~ 188/1. The best films were obtained upon GaSb (undoped) substrates. Epitaxial layers deposited on other substrates were inferior in quality compared to the GaSb substrates. As the temperature was varied from the optimum temperature, the hillock density on the films increased and the surfaces became nonspecular. As the flow ratio of TEGa/TMSb was varied from the optimum ratio, the hillock density in the deposited films increased. Metal precipitates approximately 250Å in diameter were observed in some of the films. The source of this is thought to be due to pre- and post-growth Ga flow conditions.

If TEGa were to be used, further growth condition experiments would be necessary to eliminate the formation of hillocks and metal precipitates. The occurrence of these defects would be most detrimental to any electronic devices. However, because the growth rates in these experiments were relatively low, growth of GaSb using TMGa was undertaken to increase the growth rate. TMGa has a higher vapor pressure which results in much higher growth rates.

4.4 Metal Alkyl Injection Sequence

Concurrent with the study of the effects of using TMGa as the Ga source was the study of the effect of alkyl injection sequence upon epitaxial crystal quality. It is also shown that the pre-injection of TMGa is detrimental to epitaxial crystal quality.

Films of undoped GaAs grown at 550°C on GaSb substrates which were pre-exposed for 15 seconds to the vapor of TMGa prior to growth were characterized by nonepitaxial globular surfaces. An example of this is shown in Fig. 12. For this particular film, the TMGa/TMSb ratio was 2.31 during the actual deposition process. Reduction of the TMGa/TMSb to 0.92 during the growth of GaSb appeared not only to reduce the size of the surface globules, but also to increase their density on the surface. By maintaining the TMGa/TMSb ratio at 0.92 and increasing pre-exposure time to 30 seconds prior to growth, results in epitaxial layer growth are shown in Fig. 13. Both of the epitaxial layers in Figs. 12 and 13 are Ga-rich.

Simultaneous injection of the metal alkyl reactant gases into the growth chamber at 550°C also results in epitaxial film growth on GaSb substrates. Films grown with TMGa/TMSb ratios ranging from 0.92 to 1.39 exhibit hillocks on their surfaces. The density of these hillocks seems to decrease with increasing TMGa/TMSb, i.e., a more Ga-rich growth environment. Figures 14 to 16 are the surface features of these GaSb films. The growth rate of the GaSb films increases linearly with the total hydrogen flow through the TMGa bubbler at 0°C (Fig. 6), i.e., the TMGa partial pressure. Finally, the growth rate of GaSb at 550°C as a function of H_2 flow through the $(CH_3)_3$ Ga bubbler (ccpm) at 0°C is shown in Fig. 17.

4.5 Growth Temperature and TMGa/TMSb Molar Injection Ratio

The effect of growth temperature at constant TMGa/TMSb ratio, as well as the effect of changing the TMGa/TMSb ratio at constant temperature, are examined in this section. In addition, the growth of GaSb grown at temperatures of 630°C was investigated in detail.

MRDC82-16131

Fig. 12 Ga-rich surface morphology of GaSb grown at 550°C and TMGa/TMSb = 2.31.

MRDC82-16132

Fig. 13 Ga-rich surface morphology of GaSb grown at 550°C and TMGa/TMSb = 0.92.

MRDC82-16133

Fig. 14 Surface features of GaSb grown at 550°C with simultaneous injection of metal alkyls and TMGa/TMSb = 0.92.

MRDC82-16134

Fig. 15 Surface features of GaSb grown at 550°C with simultaneous injection of metal alkyls and TMGa/TMSb = 1.1.

MRDC82-16135

Fig. 16 Surface features of GaSb grown at 550°C with simultaneous injection of metal alkyls and TMGa/TMSb = 1.39.

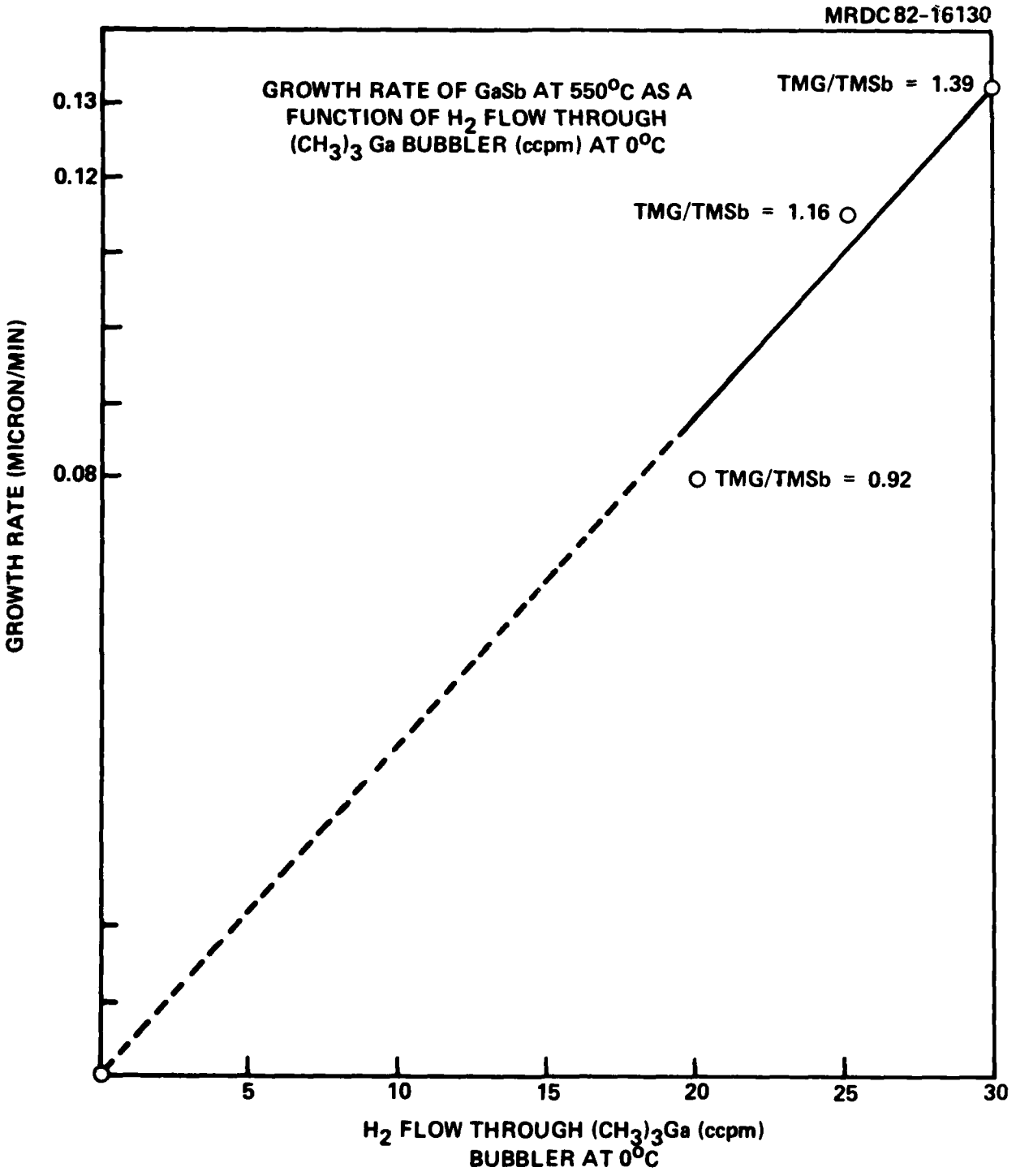

Fig. 17 Growth rate of GaSb at 550°C as a function of H_2 flow through TMGa bubbler at 0°C.

For a constant TMGa/TMSb ratio, the effect of growth temperature upon the surface morphology and reactant chemistry is clearly demonstrated by the comparison between films grown at 550°C with TMGa/TMSb = 1.16 and those grown at 600°C with the same ratio of TMGa/TMSb. Figure 18 shows the surface features of a GaSb film grown at 600°C and TMGa/TMSb = 1.16. It is characterized by round globules of excess Ga, presumably formed by the enhanced pyrolysis of TMGa at the higher growth temperature. Although the epitaxial quality of the film grown at 600°C was deteriorated relative to the 500°C growth, an approximate growth rate of ~ 0.25 μm/min was obtained. In addition, the GaSb growth rate was found to increase with temperature. Further increase in the growth temperature to ~ 630°C (TMGa/TMSb = 1.16) did not result in GaSb film formation, presumably due to improper reactant stoichiometry at the growth surface. Obviously, different stoichiometries are necessary for the different growth temperature to obtain the best films.

As the TMGa/TMSb was gradually decreased from 1.16 to 0.58 at a constant growth temperature of ~ 600°C, the GaSb surface morphology dramatically improved from a film that was characterized by surface globules to one of specular reflectivity with no whiskers or globular growth (Figs. 19, 20 and 21). The growth rate of the epitaxial GaSb grown at 600°C with TMGa/TMSb = 0.58 was 0.21 μm/min.

GaSb growth was also studied at growth temperatures ~ 630°C. Simultaneous injection of the metal alkyls at 630°C and TMGa/TMSb = 0.64 led to film surfaces characterized by tiny globules of Ga in the middle of the film surface, but smooth epitaxial growth towards the edges (Figs. 22, 23 and 24). Reduction of the TMGa/TMSb to 0.58 led to smooth epitaxial growth with occasional hillocks over the surface of the substrate (Fig. 25). Such growth was accompanied by considerable gas phase turbulence above the heated deposition zone, which could lead to nonuniform GaSb epitaxy and inhomogeneous film composition. It was not unusual to find the SiC/C susceptor and regions of the film surface covered with tiny clusters of crystalline material at the end of a growth experiment. Typical layer thicknesses were ~ 7 μm. When the

MRDC82-16136

Fig. 18 Surface features of GaSb grown at 600°C and TMGa/TMSb = 1.16.

MRDC82-16137

Fig. 19 GaSb surface morphology at 600°C with TMGa/TMSb from 1.16 to 0.58.

MRDC82-16138

Fig. 20 GaSb surface morphology at 600°C with TMGa/TMSb = 0.9.

MRDC82-16139

Fig. 21 GaSb surface morphology at 600°C with TMGa/TMSb = 0.58.

Fig. 22 Surface features of GaSb grown at 630°C and TMGa/TMSb = 0.64.

MRDC82-16146

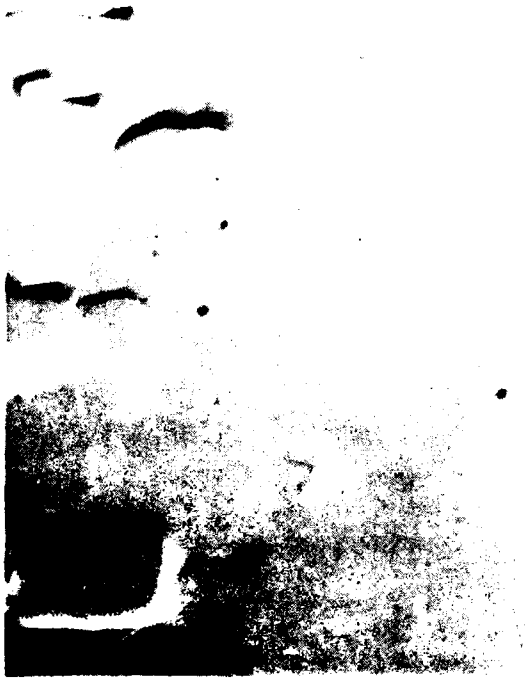

Fig. 23 Surface features of GaSb grown at 630°C and TMGa/TMSb = 0.64.

Fig. 24 Surface features of GaSb grown at 630°C and TMGa/TMSb = 0.64.

MRDC82-16148

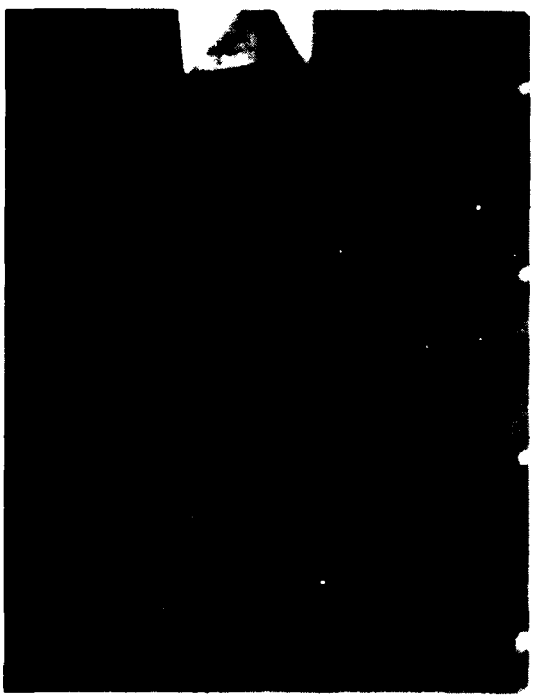

Fig. 25 Surface features of GaSb grown at 630°C and TMGa/TMSb = 0.58.

growth rate was reduced to ~ 0.1 μm/min by simultaneous reduction of both H_2/TMGa and H_2/TMSb flows while maintaining TMGa/TMSb = 0.58, the gas phase turbulence was significantly decreased. In order to reduce any thermal degradation of the GaSb substrate (MP ~ 712°C; dissociation pressure ≈ 10^{-2} Torr) during equilibration at higher growth temperatures, experiments were performed in which TMSb was injected into the growth chamber when the SiC/C susceptor first reached 550°C. The injection rate for the TMSb was ≈ 1.7×10^{-5} mole/min. This continued until the growth temperature stabilized at ~ 630°C. Studies showed that under these "pre-antimony" conditions, no elemental Sb was found to condense on the substrate surface. Thirty seconds prior to beginning the growth of GaSb, the H_2/TMSb flow rate was adjusted to insure the proper TMGa/TMSb ratio. The growth rate of GaSb using this pre-antimony procedure was slightly greater than the growth rate for GaSb grown using simultaneous metal alkyl injection procedures, i.e., 0.14 μm/min compared to 0.10 μm/min at 630°C and TMGa/TMSb = 0.58. No significant differences were noticed in the film morphology of GaSb grown using these different techniques.

4.6 Substrate Cleaning Procedure

The surface quality of undoped GaSb films was studied as a function of the substrate cleaning procedure. All of the epitaxial layers were grown at a temperature of ~ 600°C with the TMGa/TMSb ratio equal to 0.64. The films were typically 10 to 11 μm thick (growth rate ~ 0.21 μm/min). Te doped GaSb oriented 1/2° off <100> toward the <110> served as the substrate for the experiments described.

Three different cleaning procedures were evaluated. Procedure A involved simple surface degreasing techniques in 1,1,1-trichloroethane, acetone, and methanol. Reflection electron diffraction studies indicated the probable presence of a surface oxide. This oxide layer was easily removed by exposing the organically cleaned surface to hydrofluoric acid for ~ 5 minutes. Aqueous hydrofluoric acid (49%) not only removes the native oxide film, but also dissolves some of the GaSb:Te surface owing to its n-type conductivity. This HF treatment constituted the second step in Procedures B and C.

Procedures B and C differed only in the chemical nature of the oxidizing agent, which was used to break the GaSb bonds of the substrate material. Of the numerous oxidizing agents that have been used successfully with GaSb, only the Br_2-CH_3OH and Br_2-HBr systems were investigated in our study, primarily for the reasons of etch rate, purity of etchants, and mode of attack. When attacked by strong oxidizing agents, GaSb forms the insoluble trioxide and/or pentoxide on the surface. The exact oxide formed is dependent upon the strength of the oxidizing agent. In order to help eliminate this reaction, short etching times combined with rapid swirling of the etchant are required, followed by immediate washing with hydrofluoric acid. The hydrofluoric acid serves as a complexing agent to keep the Sb in solution (antimonyl ion SbO^+), and hence prevents subsequent precipitation of antimonyl-oxy salts upon dilution of the oxidizing mixture during the deionized water rinse step.

Optical microscopy photographs of GaSb films simultaneously grown at 600°C on GaSb:Te substrates, which were cleaned according to Procedures A, B and C, seemed to indicate that substrates etched in the Br_2-HBr gave film surfaces which were better than those grown on the substrates etched in Br_2-CH_3OH. However, the Br_2-CH_3OH gave good results when the HF was rinsed with CH_3OH and <u>not with</u> H_2O. The results of the three procedures are summarized in Table I.

Table I

Cleaning Procedures Evaluated for GaSb:Te Substrate Materials

Procedure A	Procedure B	Procedure C
Boiling Trichlor[a]/5 min	Hydrofluoric acid/5 min	Hydrofluoric acid/5 min
Boiling Acetone/5 min		
Boiling Methanol/5 min	1% Br_2-MeOH/15 sec	1% Br_2-HBr/10 sec
N_2 Blow Dry	Hydrofluoric acid dip	Hydrofluoric acid dip
	Deionized H_2O rinse	Deionized H_2O rinse
	Methanol dip	Isopropanol dip
	N_2 blow dry	N_2 blow dry

a. 1,1,1,-trichloroethane

4.7 Substrate Orientation and Conductivity Type as a Function of Gas Phase Stoichiometry Ratio

The surface morphology of epitaxial GaSb films grown by MOCVD at 630°C and TMGa/TMSb ratios < 0.58 (pre-antimony procedure) was found to be critically dependent upon the orientation of the GaSb substrate used in the growth. Three orientations were evaluated: 1) < 1/2° off <100>, 2) 2° off <100>, and 3) 5° off <100>. All three orientations were inclined toward the <110> direction. The substrates were Te doped, subjected to the same cleaning procedure (reference Procedure C), and subsequently evaluated by simultaneous growth of undoped GaSb (~ 6.25 μm) over a 45 minute period. The surface morphology of the layers decreased in quality in the following order: 5° off <100>, 2° off <100>, < 1/2° off <100> (Figs. 26, 27 and 28). Figure 29 illustrates the morphology of GaSb grown on undoped GaSb <100> under the same growth conditions. GaSb layers grown on GaSb:Te 5° off <100> substrate material were found to be highly reflective, very smooth, and virtually free of raised pyramidal hillocks. For these reasons, GaSb:Te 5° off <100> substrate material was used in all subsequent growth experiments.

MRDC82-16149

Fig. 26 Surface morphology of GaSb grown at 630°C on GaSb:Te < 1/2° off <100>.

MRDC82-16150

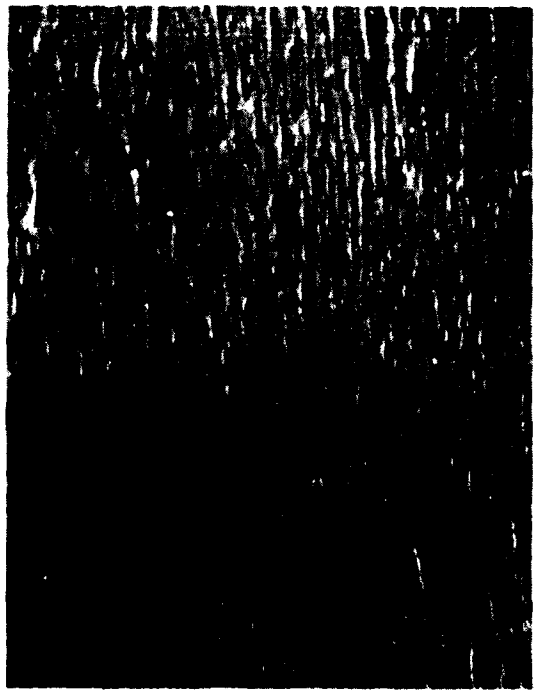

Fig. 27 Surface morphology of GaSb grown at 630°C on GaSb:Te 2° off <100>.

MRDC82-16151

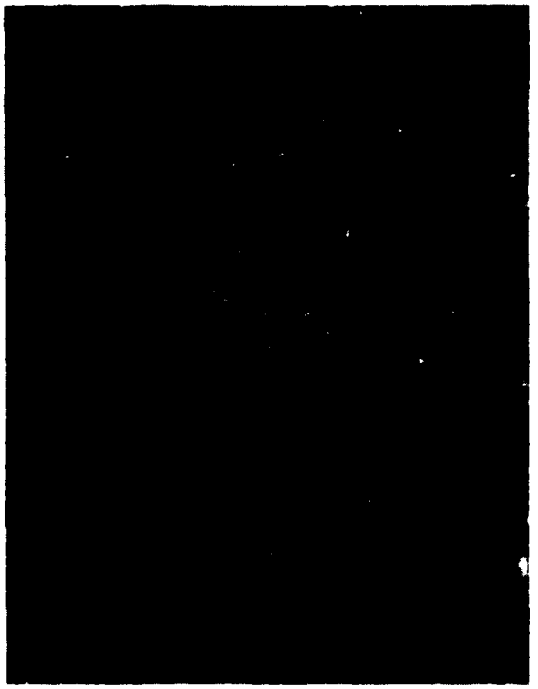

Fig. 28 Surface morphology of GaSb grown at 630°C on GaSb:Te 5° off <100>.

MRDC82-16152

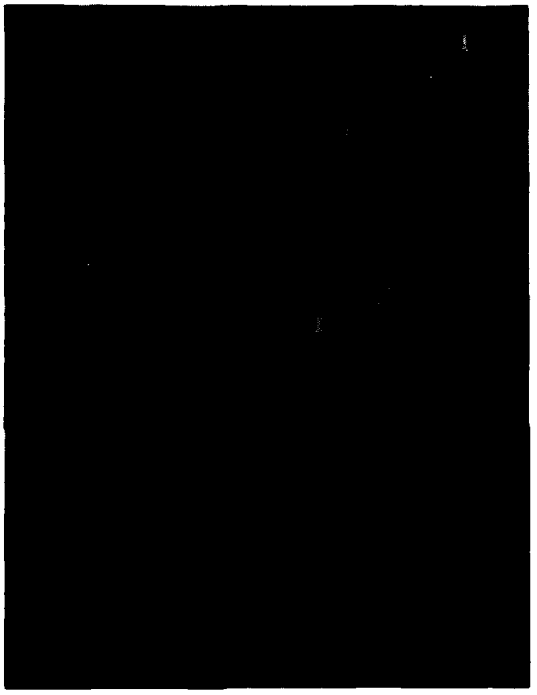

Fig. 29 Surface morphology of GaSb grown at 630°C on undoped <100> GaSb.

Eight undoped GaSb layers were grown on GaSb:Te 5° off <100> substrate material at 630°C and TMGa/TMSb ranging from 0.58 to 0.20, i.e., constant H_2/TMGa; variable H_2/TMSb. The purpose of these experiments was to study any changes in the net carrier concentration ($N_A - N_D$) within the film as a function of increasing H_2/TMSb. Since GaSb typically grows p-type, we wanted to see if there was any indication of an eventual crossover point to n-type conductivity as is commonly observed during the MOCVD growth of GaAs. However, all of the layers grown remained p-type. Preliminary hot point probe measurements indicated that the layers remained p-type over the entire range of TMGa/TMSb ratios investigated. The growth rate as a function of TMGa/TMSb ratio increased from 0.138 μm/min at TMGa/TMSb = 0.58 to 0.16 μm/min at TMGa/TMSb = 0.20. When the TMGa/TMSb ratio dropped below 0.20, the crystal growth was accompanied by whisker formation along the edges and on the surfaces of the film. Therefore, contrary to what is found in the MOCVD growth of GaAs, no conversion of conductivity type was observed for the GaSb as the Group III to Group V molar ratio was varied over a wide range.

4.8 GaAlSb Epitaxial Crystal Growth

With the GaSb crystal growth parameters established, the next phase of the program was to establish the conditions for the growth of the $Ga_{1-x}Al_xSb$ alloy upon GaSb substrates by MOCVD and to evaluate the composition of the alloy layers by double crystal x-ray diffractometry. During the course of the study, it was found that substrate cleaning procedures had a substantial effect upon the final surface morphology of the $Ga_{1-x}Al_xSb$ film. Procedure C, as outlined in Section 4.6, was used with the CH_3OH final rinse.

The conditions for the growth of $Ga_{1-x}Al_xSb$ upon GaSb were similar to that of GaSb upon GaSb. TMGa, TMSb and TMAl are used as the sources of Ga, Sb and Al, respectively. The TMGa and TMSb were kept at 0°C, while the TMAl was kept at room temperature.

A typical growth procedure is now described. Following substrate preparation, the sample was loaded into a clean quartz reactor containing a

clean silicon carbide-coated susceptor. The reactor was pumped to 1 μm of pressure and then backfilled with flowing H_2 gas. When the reactor reached atmospheric pressure, the flow rate of H_2 gas was increased from 2 ℓ/min to 7 ℓ/min. After a minimum of 15 minutes of purging in the dry H_2 ambient, the susceptor was heated to 625°C-650°C for one minute and then stabilized at 625°C. The heat-up and stabilization process typically required 15 minutes. During this time, the H_2 flowing through the metalorganic bubblers was allowed to reach equilibrium. After temperature stabilization, a 4 μm thick buffer layer of GaSb was deposited upon the substrate. This was followed by the growth of 2 to 3 μm of $Ga_{1-x}Al_xSb$. Prior to the injection of the alkyls for the ternary growth, the reactor was purged for 20 seconds with pure H_2 gas to remove all of the AsH_3. After the growth of the $Ga_{1-x}Al_xSb$ layer, the wafer was allowed to cool to room temperature in a hydrogen ambient.

During the growth of the $Ga_{1-x}Al_xSb$ ternary, the H_2 flow rates through the TMGa and TMSb were held constant at 15 ccpm and 66 ccpm, respectively. The H_2 flow rate through the TMAl bubbler was varied from 8 ccpm to 60 ccpm. Assuming saturation of the H_2 gas as it passed through the bubbler, the molar amount of metal alkyl can be calculated with

$$n_i = \frac{[e^{2303(A-BT)^{-1}}](\text{flow rate } H_2)}{RT} \quad , \tag{3}$$

where A and B are constants characteristic of each metal alkyl. Shown in Fig. 30 is the aluminum content in the film as a function of TMAl/TMGa molar ratio. The full width half maximum of the x-ray intensity peak increased as the ratio of TMAl/TMGa increased. At a composition of $Ga_{1-x}Al_xSb$ ($x \sim 0.37$), the FWHM increased by a factor of two relative to the substrate. One other point should be mentioned; beyond the $x \sim 0.37$, further increases in the H_2 flow through TMAl bubblers did not increase the AlSb mole fraction in the film. This implies that the growth conditions must be changed to increase the AlSb mole fraction in the film. When the flow rate through the TMAl bubbler was increased beyond that which was necessary for $x \sim 0.37$, the film composition

MRDC82-17937

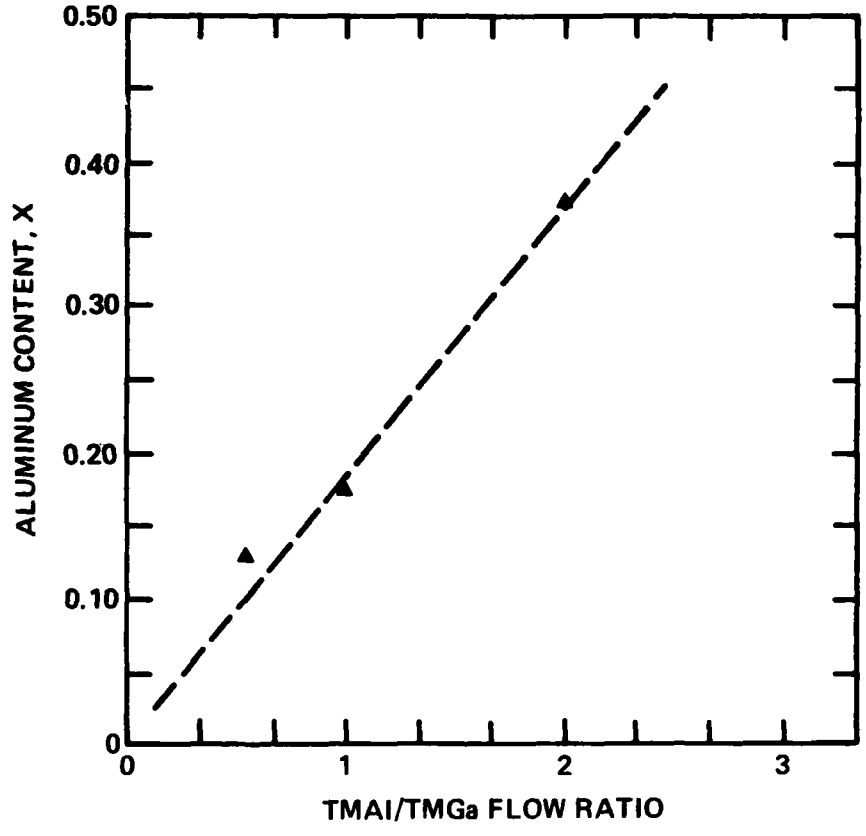

(a) DOUBLE CRYSTAL X-RAY DIFFRACTOMETRY

Fig. 30 AlSb solid mole fraction as a function of TMAl/TMga molar gas ratio.

of $Ga_{1-x}Al_xSb$ remained at an AlSb mole fraction of $x \sim 0.37$. This indicated that perhaps a rate limiting reaction is occurring or that competition is occurring between Column III species.

In order to eliminate the competition between the Al and Ga species for the Column III sites, the H_2 flow through the TMGa bubbler was stopped. Following crystal growth, the AlSb films were characterized by double crystal x-ray diffraction for crystalline quality. X-ray line broadening of the AlSb film by a factor of nine occurred relative to the x-ray linewidth of the GaSb substrate. In addion, the peak intensity of AlSb was five time lower than expected for this film thickness. X-ray line broadening has also been seen to occur in GaAlAs grown at low temperatures (< 700°C). The broadening is attributed to the enhanced incorporation of oxygen at low growth temperatures. It is for this reason that GaAlAs is typically grown at 750°C rather than 600°C. It is probable that the same O_2 incorporation phenomenon is occurring in the growth of AlSb at $T_g \sim 625°$.

This phenomenon has crucial implications for aluminum-containing alloys which require low growth temperatures. Examples would be InP/InGaAlAs heterostructures, where InP has high vapor pressures, or structures with low melting point substrates such as InSb. This incompatibility of growth temperature requirements points out the need to investigate low growth temperature processes which require aluminum.

For this program, the GaAlSb layers required AlSb mole fractions of 0.30 or less. No further investigations of GaAlSb were made.

4.9 Growth of GaAsSb Upon GaSb and InAs Substrates

Following the completion of the GaAlSb work, efforts were directed toward establishing the conditions necessary for deposition of epitaxial layers of GaAsSb onto GaSb and InAs substrates using the MOCVD technique. The conditions necessary to prevent InAs decomposition prior to epitaxial deposition were investigated. Deposition was examined at temperatures of 550°C, 585°C and 625°C. During the course of the experimentation, it was determined

that As incorporation into the crystal lattice in the presence of Sb was enhanced by over an order of magnitude. The above findings and conditions are now discussed in detail.

The substrate material was Te doped <100> GaSb oriented 5° toward the <110> and Sn doped <100> InAs. During all experiments, seven liters of Pd-purified hydrogen flowed through the reaction chamber. The sources of Ga and Sb were TMGa and TMSb, respectively; the source of As was arsine (AsH_3, 10% in UHP-H_2).

In order to prevent InAs substrate decomposition at high growth temperature, yet achieve GaAsSb layers with low solid fractions of As, two electronic mass flow controllers were used to regulate the quantity of AsH_3/H_2 being injected into the reactor chamber.

High AsH_3/H_2 flows were regulated with a mass flow controller calibrated for 0 to 500 sccm AsH_3/H_2. This flow range corresponds to 0 to 2.23×10^{-3} moles of AsH_3 per minute. The primary purpose of this particular controller was to provide sufficient AsH_3 overpressure to help minimize InAs substrate decomposition prior to growth of the $Ga_{1-x}Al_xSb$ alloy layer, as mentioned previously, and also to maintain an adequate supply of AsH_3 in the reactor chamber during the cool-down cycle following a deposition. The vacuum decomposition temperature for InAs is ~ 720°C; the decomposition pressure of InAs is approximately equvalent to ~ 0.33 atm of As at 940°C.

Low flows of AsH_3/H_2 were controlled with a mass flow controller calibrated for 0 to 32.3 sccm AsH_3/H_2. This flow range corresponds to 0 to 1.45×10^{-4} mole of AsH_3 per minute. The primary purpose of this controller was to provide precise control of the amount of AsH_3 being injected into the reactor chamber during the growth of the $Ga_{1-x}Al_xSb$ alloy material. Small changes in the AsH_3/TMSb being injected into the reactor chamber would be expected to drastically effect the amount of Sb and As incorporated into the alloy lattice at a given growth temperature. For this reason, the AsH_3/H_2 was premixed wth the metalorganic source materials in a mixing manifold just above the entrance to the reactor chamber. Efficient mixing of all the reactants

was achieved by using 7 LPM UHP-H_2. This enabled uniform control and mixing of the reactant gases throughout the growth process.

Preliminary first order calculations (Appendix IV) indicated that, in order to achieve approximately 10% As incorporation into the $Ga_{1-x}Al_xSb$ alloy, it would be necessary to inject ~ 17×10^{-6} mole/min of AsH_3 into the growth chamber, the exact amount being dependent on the TMGa/TMSb. This quantity of AsH_3 corresponds to ~ 4 sccpm of AsH_3/H_2 flow. In practice, the actual flow of AsH_3/H_2 required was expected to be greater than the calculated 4 sccm due to the incomplete pyrolysis of AsH_3 and the subsequent As incorporation inefficiency, which was expected to be less than 100% at these conditions of growth.

For the growth of GaAsSb on InAs substrates, the InAs substrates were cleaned using a procedure analogous to that used with GaSb substrates. Substrate orientation was <100>.

Since the crystal growth experiments utilized InAs substrates, it was necessary to establish what minimum amount of AsH_3 overpressure would be required to minimize (or prevent) surface decomposition prior to growth of the alloy material at ~ 625°C. Table II summarizes the steps taken during a typical growth sequence.

Table II

$GaAs_{1-x}Sb_x$ Growth Sequence

- Clean substrates and load into reactor chamber.
- Evacuate reactor chamber 30 min at $\leq 10^{-3}$ Torr.
- Backfill reactor chamber with UHP-H_2 at 7 LPM.
- Commence rf heating of SiC/C substrate holder.
- Inject AsH_3/H_2 at 500° into reactor chamber.
- Equilibrate at growth temperature and commence substrate rotation.
- Pre-trimethylantimony injection 30 seconds.
- Trimethylgallium injection and commence alloy growth.
- Simultaneously stop metal alloy flows to the reactor.
- Maintain AsH_3/H_2 flow and terminate rf heating.
- Cool to ambient in AsH_3/H_2.
- Divert AsH_3 to exhaust and continue flushing reactor chamber with UHP-H_2.
- Turn off UHP-H_2 to exhaust and remove sample.

During the first experiment, 10 sccm of AsH_3/H_2 ($\sim 4.5 \times 10^{-5}$ mole/min AsH_3) was found to be inadequate to prevent substrate decomposition during the growth of the alloy layer. AsH_3/H_2 (10 sccm) was injected into the reactor chamber at 550°C during the heating phase. No apparent decomposition of the substrate was observed as the temperature increased from 500°C to 625°C. After equilibration at 625°C, H_2/TMSb was introduced into the reactor chamber, followed by (30 seconds) injection of H_2/TMGa; the TMGa/TMSb = 0.35. This procedure provides a Group V rich (TMSb + AsH_3) environment surrounding the substrate prior to injection of the TMGa into the reactor chamber. Owing to the high total flow of gas past the heated susceptor, film growth begins within seconds following injection of the H_2/TMGa. The growth surface remained highly reflective for approximately 2 min, but quickly degraded to a hazy surface characterized by a dense population of raised molten areas. These

areas were not round or globular (as in the case of excess Ga) and were thought to be In metal (Fig. 31). Although no attempt to confirm this speculation was made, they exhibited the same structural characteristics of an InAs surface which had been heated to ~ 625° in the absence of AsH_3. The same type of features present here have also been observed on InP which has undergone slight thermal decomposition. Increasing the AsH_3/H_2 flow to 32 sccm (~ 14.3×10^{-5} mole/min) and repeating the previous experiment resulted in epitaxial film growth. After 30 minutes of epitaxial deposition, the surface was slightly hazy. Optical examination revealed the presence of occasional pyramidal hillocks on an otherwise smooth surface. The growth rate in this experiment was ~ 0.13 μm/min.

Although the quantity of AsH_3 (14.3×10^{-5} mole/min) used in the previous experiment was capable of preventing substrate decomposition during the growth cycle, it was approximately eight times the amount originally calculated for $GaAs_{0.10}Sb_{0.90}$. Four additional growth experiments were performed during which the AsH_3/H_2 flow rate was systematically increased while maintaining the TMGa/TMSb constant at 0.35. Table III summarizes the growth parameters used during these experiments. The molar injection rates of AsH_3 used in these growths ranged from 1.43×10^{-4} to 17.9×10^{-4} mol/min. Growth rates were constant at ~ 0.3 μm/min.

All the films were analyzed by energy dispersion x-ray analysis (EDAX) prior to any x-ray techniques. No Sb was detected in any of the films. A 4.7 μm film of GaAs was then grown on an InAs substrate at ~ 625°C using AsH_3/TMGa = 30.3. The relative Ga/As ratio determined by EDAX was found to be identical to the GaAs ratio determined for the alloy growths previously described in which no Sb was detected. This result qualitatively indicates these films to be GaAs.

MRDC82-16459

Fig. 31 GaAsSb/InAs heteroepitaxial showing In upon the surface.

Table III

$GaAs_xSb_{1-x}$ Growth Experiments at 625°C[a]

Growth Rate µm/min	AsH_3/TMSb	AsH_3/TMGa	TMGa/(AsH_3 + TMSb)	EDAX Measurement
0.127	0.828	2.392	0.190	No Sb; Ga,As present
0.106[b]	1.294	3.731	0.151	No Sb; Ga,As present
0.127	2.588	7.463	0.100	No Sb; Ga,As present
0.127	5.176	14.925	0.056	No Sb; Ga,As present
0.127	10.55	30.303	0.031	No Sb; Ga,As present

a. TMGa/TMSb = 0.35

b. Poor cleave

The growth rate for the 'pure' GaAs growth was 0.156 µm/min, which is slightly greater than the 0.127 µm/min observed for the films grown in the presence of TMSb. It is possible to speculate that the 'alloy' growth rate is reduced due to competing side reactions between the TMSb and AsH_3, i.e.,

$$(CH_3)_3Sb + AsH_3 \overset{\Delta}{\Leftrightarrow} (CH_3)_3As + SbH_3 \quad . \tag{4}$$

Such reactions would tend to reduce the available AsH_3 which is reacting with the TMGa to form GaAs. It should also be pointed out, however, that this effect appears to be constant over a wide range of H_2/TMSb flow rates, i.e., the same growth rate ~ 0.13 µm/min is observed for H_2/TMSb flows of 25, 50 and 100 sccm with a constant AsH_3/H_2 flow rate.

In order to verify that the EDAX mode on the SEM was working properly for samples containing Sb, a previously grown sample of GaSb/InAs was submitted for EDAX analysis. The results confirmed the compostion of GaSb.

From these preliminary findings, no x-ray analysis was performed on any of the alloy growth films.

In order to determine whether it was possible to incorporate Sb into the solid, the effect of growth temperature had to be examined. Previous experimental data had shown that a gradual decrease in the Sb incorporation during the growth of $GaAs_xSb_{1-x}$ films occurs as the temperature is increased from 500°C to 630°C. Workers at Varian Associates proposed that a kinetic balance exists between the As and Sb atoms relative to basic atomic incorporation mechanisms such as atomic surface mobility. Therefore, at some growth temperature lower than 625°C, a boundary between surface kinetically controlled growth and mass transport limited growth of this material should occur. Once the temperature is reduced below some critical temperature, T_c, the incorporation of Sb is greatly enhanced.

Although we have not yet investigated in any detail the effect of growth temperature on Sb incorporation in $GaAs_xSb_{1-x}$ alloy films grown by MOCVD on InAs substrates, three preliminary deposition experiments were performed at 550°C. These experiments will now be described. A summary of the growth parameters is presented in Table IV.

Table IV

$GaAs_xSb_{1-x}$ Growth Experiments at 550°C

Growth Rate µm/min	AsH_3/TMSb	AsH_3/TMGa	TMGa/(AsH_3 + TMSb)	EDAX Measurement
0.06	1.294	3.73	0.151	No Sb; Ga,As present
Powder Surface	10.35	30.30	0.031	---
Powder Surface	2.59	3.73	0.192	No Sb; Ga,As present

During the first experiment, AsH_3 (22.5×10^{-5} mole/min) was injected into the growth chamber at 500°C. After equilibration at 550°C, H_2/TMSb (100 ccpm) was introduced for 30 seconds, followed by H_2/TMGa. the TMGa/TMSb ratio = 0.34. The film surface remained reflective for 30 minutes at which time the growth was terminated. The film thickness was only 1.88 μm (~ 0.067 μm/min). EDAX analysis of the film indicated the absence of Sb. Ga and As were present.

When the above experiment was repeated with higher AsH_3/H_2 flows corresponding to ~ 90×10^{-5} mole/min, polycrystalline GaAs formed on the surface of the InAs substrate.

Polycrystalline GaAs was again formed on the surface of the InAs when the first experiment was repeated following a reduction in the H_2/TMSb flow to half the original value. The reduction in H_2/TMSb would have 'effectively' increased the localized AsH_3 concentration at the growth zone resulting in the formation of polycrystalline GaAs.

Initial attempts to grow $GaAs_xSb_{1-x}$ ($x \sim 0.10$) at 625°C, TMGa/TMSb = 0.34, and AsH_3 molar flow rates of 1.43×10^{-4} mole/min resulted in formation of GaAs. The results suggest additional studies using AsH_3 flows $< 1.4 \times 10^{-4}$ mole/min at 625°C and TMGa/TMSb = 0.34 are necessary, as well as using AsH_3/H_2 source mixtures less than 10% in volume concentration. It appears necessary to grow $GaAs_xSb_{1-x}$ layers at growth temperatures less than 625°C in order to avoid InAs substrate decomposition problems.

At this point, it became necessary to determine whether the necessary conditions to grow epitaxial GaAsSb by MOCVD could be established. In order to isolate the problem, GaAs 5° off the <100> was chosen as the substrate to establish calibration curves. The growth conditions were the same as those which produced the best GaSb, except 1% AsH_3 in H_2 was added to the gas stream in various amounts. The H_2/TMGa flow and H_2/TMSb bubbler flows were maintained at 15 and 100 ccpm, respectively. This corresponds to a TMGa/TMSb molar ratio of 0.34. Both bubblers were kept at 0°C. The relative amounts of As to Sb in the solid were determined by EDAX. A plot of the solid

composition as a function of μmoles of AsH_3/min is shown in Fig. 32. This demonstrated that GaAsSb could be epitaxially grown by MOCVD.

Having established that GaAsSb could be grown by MOCVD and that the approximate stoichiometry of gases necessary to grow $GaAs_xSb_{1-x}$ with $x \sim 0.10$ was known, work was resumed upon the growth of epitaxial $GaAs_{1-x}Sb_x$ upon InAs. From the previous experiments of GaAsSb grown on InAs at 620°C, the next step was to reduce the growth temperature to 580°C. This would still permit substantial pyrolysis of arsine to occur. The initial growth conditions of GaAsSb upon InAs were similar to the conditions of GaAsSb upon GaSb. Flows of H_2 through the TMGa and TMSb bubblers were 15 and 100 ccpm, respectively. Both bubblers were kept at 0°C. The InAs substrate was cleaned using organic solvents and then etched using Br:Meth (1% Br). The AsH_3 (104 ccpm, 4.64×10^{-5} moles) was injected into the reactor vessel at 400°C for stabilization. The sample was allowed to equilibrate at 580°C for 15 minutes prior to the injection of the metal alkyls. No visible surface degradation was observed. Following the injection of the metal alkyls, raised globules began appearing on the wafer surface. This occurred over the entire sample in 15 minutes. Under microscopic examination, the raised portions did not exhibit crystalline features, but rather molten shapes. The appearance was similar to In left on an InP wafer grown by LPE. This was previously noted to occur at 620°C.

In order to eliminate the possibility of substrate decomposition, the arsine overpressure (arsine pressure prior to GaAsSb epitaxial deposition) was increased by increasing the flow rate to 500 ccpm of 1% AsH_3/H_2. The same stabilization procedure was followed, and the arsine flow was kept at a high rate until 0.35 μm of GaAsSb had been grown. The arsine flow was then reduced to 104 ccpm. The epitaxial layer remained specular much longer and exhibited crystalline features on the surface and only an occasional molten feature at the edges.

At this time, it was thought that the substrate was interacting with the incoming alkyls and forming an intermediate compound. The most likely

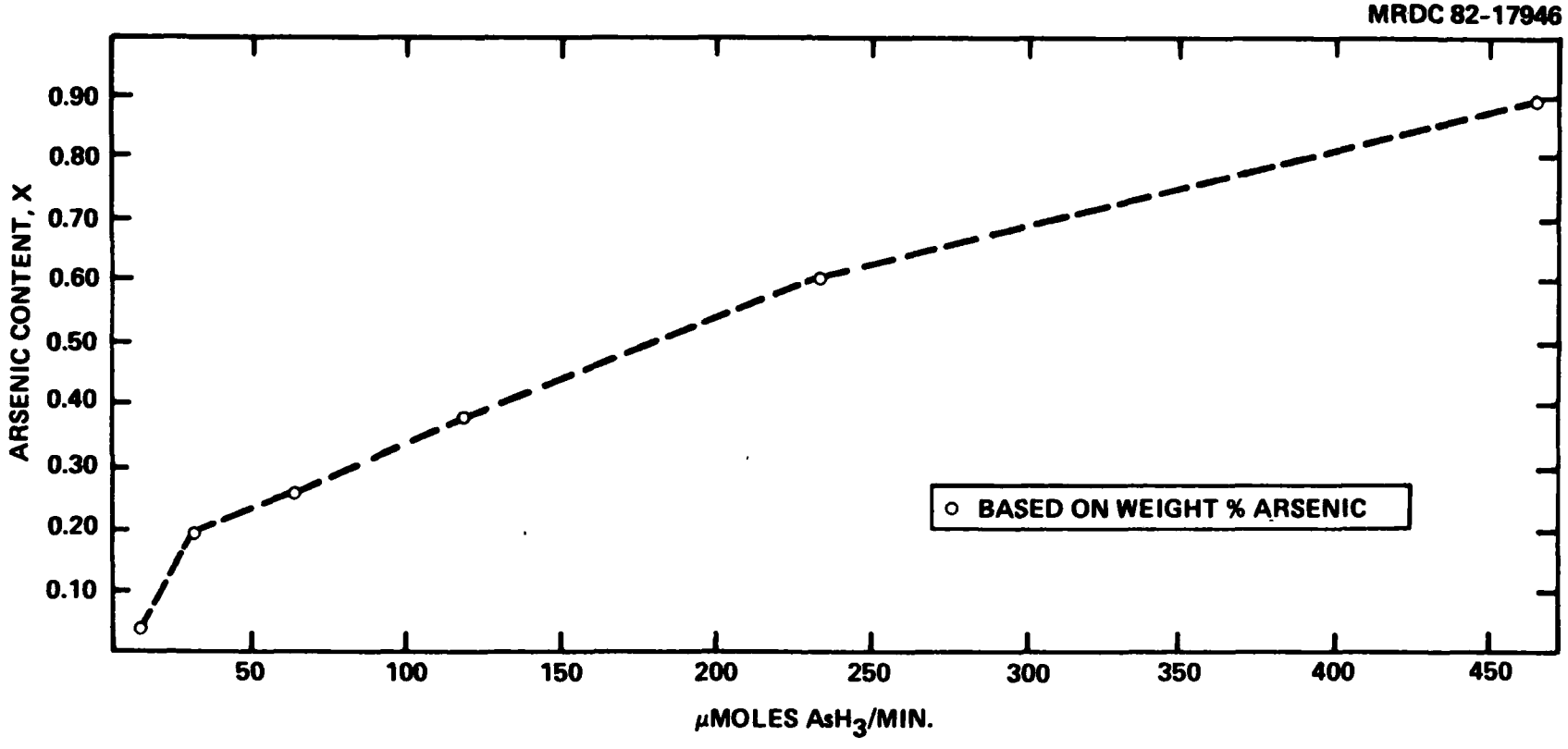

Fig. 32 GaAsSb solid composition as a function of input AsH_3 volume/min.

intermediate candidate was InSb which could then decompose due to its low melting temperature. With insufficient As overpressure, it is possible that the thermal decomposition of the substrate surface would create nucleation and substrate/film interface problems whenever film growth commenced. The reaction occurring would be

$$\text{InAs (substrate)} + (CH_3)_3Sb \text{ (adsorbed)} \xrightarrow[\Delta]{H_2} \text{InSb} + (CH_3)_3As$$
$$\text{InSb} \xrightarrow[\Delta]{H_2} \text{decomposition products (InSb m.p.} \sim 525^\circ C) \qquad (5)$$

To obviate this chemical reaction, the growth temperature was reduced from 580°C to approximately 550°C. Flow conditions for lattice-matched crystal growth at 550°C are different from those at 580°C, therefore requiring recalibration of the Sb/As source flow rate ratio. For the initial growth at 550°C, the flow rates through the TMGa and TMSb bubblers were 15 and 40 ccpm, respectively. The bubblers were kept at 0°C. The main manifold rate was kept at 7 ℓ/min of H_2. Following the same stabilization procedure as at the higher temperature of 580°C, after equilibration the reactor chamber was purged of AsH_3 for 60 seconds. This was followed by a 60 second or 600Å growth of GaSb. GaAsSb alloy was then grown for 60 minutes using 10 ccpm (1% AsH_3/H_2). No decomposition of the wafer was observed at this growth temperature. Hillocks were still present; however, their density was much reduced as compared to the higher temperature growth. An example of the surface is shown in Fig. 33. Changing the ratio of Sb/As by decreasing the AsH_3 flow to 5.0 ccpm (1% AsH_3/H_2) reduced the hillock density further, as evident in Fig. 34. A change of the TMGa/TMSb ratio from 0.86 to 1.15 decreased the hillock density still further, as shown in Fig. 35. Further increase of the TMGa/TMSb ratio to 1.73 increased the hillock density.

In an attempt to identify the source of the hillocks in the epitaxial layer, InAs substrates were subjected to the stabilization procedure employed in our crystal growth, followed by the growth of 600Å of GaSb. The variable parameter was the temperature at which the AsH_3 was introduced into the

MRDC82-20953

Fig. 33 GaAsSb/InAs heteroepitaxy with TMGa/TMSb molar ratio = 0.86, AsH_3 = 2.9 μmole/min and T_g = 550°C.

MRDC82-20952

Fig. 34 GaAsSb/InAs heteroepitaxy with TMGa/TMSb molar ratio = 0.86, AsH_3 = 0.03^2 ccpm (1.34 μmole/min).

MRDC82-20951

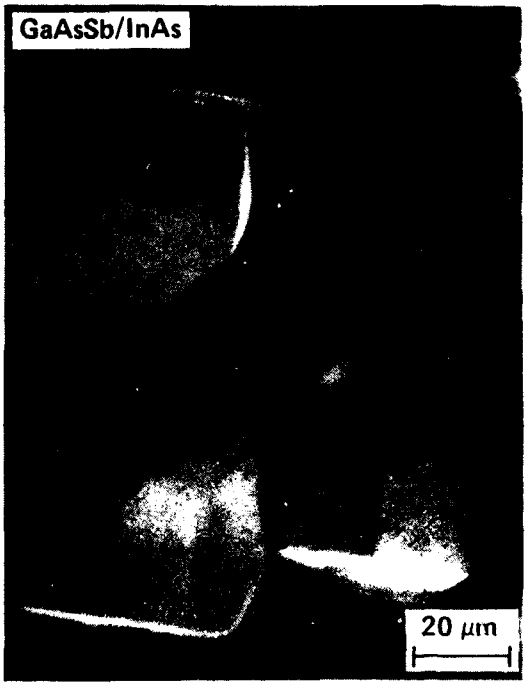

Fig. 35 GaAsSb/InAs heteroepitaxy with TMGa/TMSb molar ratio = 1.15, AsH_3 = 2.9 μmole/min.

reactor chamber during the heating phase. It was found that even with injection of AsH_3 occurring at 400°C, some defects decorated the surface, as shown in Fig. 36a. A substantial reduction of the defects occurred with the injection of AsH_3 at room temperature (see Fig. 36b). These experiments demonstrate that the InAs substrates currently in use are one source of the defects observed in the epitaxial layers.

The results of this section are readily summarized in Fig. 37 which shows the surface morphology of the $GaAs_xSb_{1-x}$/InAs heterostructures at selected growth temperatures and AsH_3 overpressures.

The GaAsSb/InAs heterostructures were examined using double crystal x-ray diffraction. From these measurements, it was determined that $GaAs_xSb_{1-x}$ could be lattice-matched under the following conditions:

- Growth temperature = 550°C
- Pre-AsH_3 at 220 μmole/min at 25°C
- AsH_3 flow at 20 μmoles/min
- $(CH_3)_3Ga/(CH_3)_3$ Sb ratio = 1.15

Epitaxial layers grown under these conditions exhibited high crystalline quality.

The effects of lattice mismatch upon the x-ray linewidth of the epitaxial film is shown in Fig. 38. Figure 38a shows the rocking curve of a GaAsSb film with $\Delta a/a = 1.8 \times 10^{-3}$, while Fig. 38b shows a GaAsSb film having $\Delta a/a = 2.8 \times 10^{-3}$. The rocking curve of Fig. 38b is noticeably broader than the curve of Fig. 38a. This is not caused by any growth condition phenomenon or grading, but rather is related to film strain. The film of Fig. 38a is under compression, while that of Fig. 38b is under tension. Work on InGaAs/GaAs has shown that films under tension exhibit poorer crystalline quality. In fact, when a film is under sufficient tension, it will eventually fracture. Therefore, films of GaAsSb, if not lattice-matched to InAs, should be grown under compression to produce higher crystalline quality.

PRE AsH_3 AT 400°C
220 μMOLE/MIN.
60 SECOND AsH_3 PURGE
60 SECOND GaSb GROWTH
COOL IN H2

PRE AsH_3 AT 25°C
220 μMOLE/MIN.
60 SECOND AsH_3 PURGE
60 SECOND GaSb GROWTH
COOL IN H2

PRE AsH_3 AT 25°C
220 μMOLE/MIN.
60 SECOND AsH_3 PURGE
COOL IN H2

Fig. 36 Effect of pre-AsH_3 initiation temperature on buffer layer grown on InAs at 550°C.

MRDC82-17930

PRE AsH_3 AT 450 μMOLE/MIN.
GROWTH AsH_3 AT 46 μMOLE/MIN.

$GaAs_xSb_{1-x}$/InAs AT 620°C

InAs SURFACE DEGRADATION AT 620°C

PRE AsH_3 AT 220 μMOLE/MIN.
GROWTH AsH_3 AT 46 μMOLE/MIN.

$GaAs_xSb_{1-x}$/InAs AT 580°C

InAs "EDGE" DEGRADATION AT 580°

PRE AsH_3 AT 220 μMOLE/MIN.
GROWTH AsH_3 AT 1.4 μMOLE/MIN.

$GaAs_{.06}Sb_{.94}$/InAs AT 550°C

Fig. 37 Surface morphology of GaAsSb/InAs heteroepitaxy.

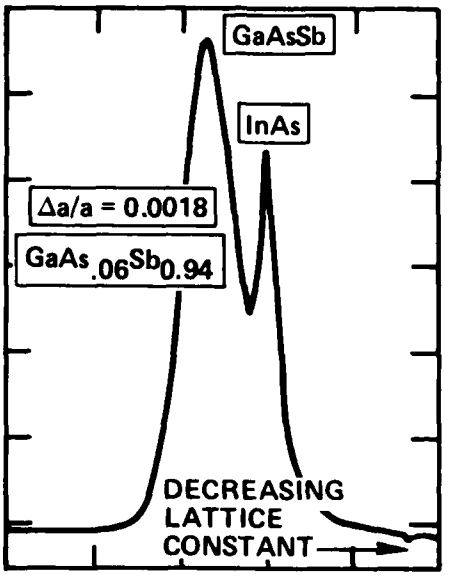

$GaAs_xSb_{1-x}$/InAs GROWN
WITH 1.4 μMOLE/MIN. AsH_3

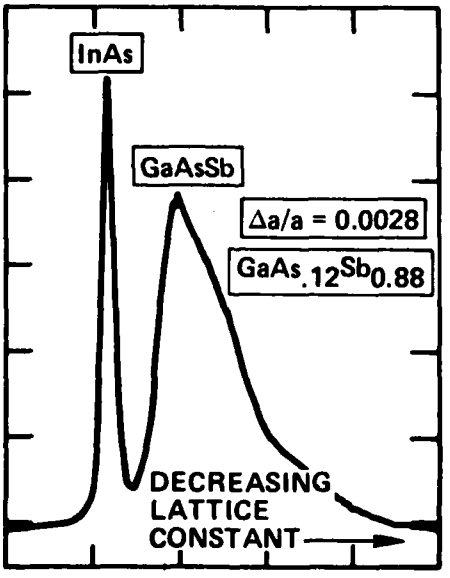

$GaAs_xSb_{1-x}$/InAs GROWN
WITH 2.9 μMOLE/MIN. AsH_3

Fig. 38 X-ray rocking curves of GaAsSb/InAs under compression (upper curve) and tension (lower curve).

4.10 N-Type GaSb Doping and Schottky Barrier Photodetectors

The MOCVD growth of *n*-type films of GaSb was also investigated. Initially, GaAs films doped with Se were grown in order to calibrate the 1% $H_2Se:H_2$ dopant source. GaAs epilayers were grown with doping ranging from mid 10^{15} to $10^{18}cm^3$.

Having calibrated the dopant source, the goals of the GaSb doping experiments were threefold.

1. Demonstrate n-type films of GaSb grown by MOCVD.
2. Optimize the gas phase stoichiometry ratio of TMGa/TMSb to obtain the highest mobility material at a given dopant level.
3. Establish a gas phase to solid phase dopant incorporation curve. Owing to the unavailability of semi-insulating GaAs, the data required are not easily obtained.

The initial experiments demonstrated that n-type GaSb could be successfully grown by MOCVD. From Hall measurements performed on an n-type GaAs epilayer grown upon semi-insulating GaAs, a carrier concentration of $N_D-N_A \sim 1 \times 10^{17}cm^{-3}$ was obtained. The measured 300K Hall mobility was only 357 $cm^2/V\text{-sec}$. Due to the low mobility value obtained, a decision was made to characterize n-type GaSb grown upon undoped (p-type) GaSb substrates. In this way, interfacial phenomena produced by the lattice mismatch are eliminated. The data obtained from Hall measurements on these samples were inconclusive due, most likely, to the fact that the p-substrate could not be grounded during the measurement.

An alternate method of epilayer-substrate isolation was devised which consisted of growing an undoped AlSb buffer layer 1 μm thick prior to deposition of the n-type GaSb. The GaSb/AlSb/GaSb (substrate) sample was grown under slightly different conditions from the GaSb/GaAs:Cr sample. Characterization by Hall measurement indicated a carrier concentration, N_D-N_A, of $2 \times 10^{17}cm^{-3}$ with a mobility of 1200 to 1250 $cm^2/V\text{-sec}$ at 300K. For a sample

of GaSb/AlSb/GaSb (substrate) grown with the same conditions as the above described GaSb/GaAs:Cr sample, a p-type carrier concentration of $1 \times 10^{18}cm^{-3}$ was obtained. Due to the large dispersion in the data, no conclusion could be drawn about the influence of growth conditions on the quality of the epilayer.

Finally, Schottky barriers were also deposited upon n-type MOCVD grown GaSb. The breakdown voltages of these devices indicated n-type doping densities of mid $10^{17}cm^{-3}$. Photoresponse was observed on these devices. The photoresponse indicates that antimonide containing semiconductors grown by MOCVD can be fabricated into opto-electronic electronic devices.

5.0 CONCLUSIONS AND RECOMMENDATIONS

As a result of this program, we have demonstrated that through MOCVD, high quality antimonide III-V semiconductor material can be fabricated. We have shown:

- High quality hillock-free GaSb can be grown on off-orientation <100> 5° → <110> GaSb substrates.
- High quality GaAlSb ternary alloys with AlSb mole fractions of up to $x \sim 0.37$ can be grown by MOCVD.
- Schottky barrier photodetectors have been fabricated from n-type MOCVD grown GaSb.
- High quality GaAsSb/InAs heterostructures have been grown at 550°C.

The successful growth of high crystalline quality antimonide-based material by the MOCVD process and the demonstration of Schottky barrier photodetectors based upon these materials make this crystal process a viable alternative to conventional means of producing antimonide-based devices. Further research must be conducted to examine, in greater detail, the electrical and optical characteristics of the materials produced. Such efforts would be directed toward studies of GaAsSb/InAs heterostructures to determine the direct-indirect transition. In the materials area, more innovative research is necessary to devise a means of producing high quality Al-bearing alloys at low temperatures. Finally, the work performed here indicates that long wavelength heterostructures ($\lambda > 2.0$ μm) can be produced by the MOCVD process, and should be further researched for devices operating in this region.

6.0 REFERENCES

1. T. Miya, Y. Gerunuma, T. Hosaka and T. Miyashita, Electron. Lett. 15, 106 (1979).

2. T. Wao, S. Ogawa and S. Maruyama, Jpn. J. Appl. Phys. 16, 1875 (1977).

3. S. Maruyama, T. Wako and S. Ogawa, Jpn. J. Appl. Phys. 17, 1695 (1978).

4. M. Yano, Y. Suzuki, T. Ishii, Y. Matsushima and M. Kimata, Jpn. J. Appl. Phys. 17, 2091 (1978).

5. H. Sakaki, L.L. Chang, R. Lueke, C.A. Chang, G.A. Sai-Halasz and L. Esaki, Appl. Phys. Lett. 31, 211 (1977).

6. C.A. Chang, R. Lueke, L.L. Chang and L. Esaki, Appl. Phys. Lett. 31, 759 (1977).

7. A.Y. Cho, H.C. Casey, Jr. and P.W. Foy, Appl. Phys. Lett. 30, 397 (1977).

8. R.D. Dupuis and P.D. Dapkus, Appl. Phys. Lett. 31, 466 (1977).

9. R.D. Dupuis and P.D. Dapkus, Appl. Phys. Lett. 31, 839 (1977).

10. R.D. Dupuis and P.D. Dapkus, Appl. Phys. Lett. 32, 473 (1978).

11. R.M. Kolbas, N. Holonyak, R., R.D. Dupuis and P.D. Dapkus, Pisma Zh. Tekh. Fiz. 4, 69 (1978), [Sov. Tech. Phys. Lett. 4, 28 (1978)].

12. R.D. Dupuis, P.D. Dapkus, N. Holonyak, Jr., E.A. Rezek and R. Chin, Appl. Phys. Lett. 32, 295 (1978).

13. R.D. Dupuis and P.D. Dapkus, Appl. Phys. Lett. 32, 406 (1978).

14. R.D. Dupuis and P.D. Dapkus, Appl. Phys. Lett. 33, 68 (1978).

15. N. Holonyak, Jr., R.M. Kolbas, R.D. Dupuis and P.D. Dapkus, Appl. Phys. Lett. 33, 73 (1978).

16. R.D. Dupuis, P.D. Dapkus, R.M. Kolbas and N. Holonyak, Jr., Sol. State Comm. 27, 531 (1978).

17. R.D. Dupuis, P.D. Dapkus, R.M. Kolbas, N. Holonyak,Jr. and H. Shichijo, Appl. Phys. Lett. 33, 396 (1978).

18. H. Shichijo, R.M. Kolbas, N. Holonyak, Jr., R.D. Dupuis and P.D. Dapkus, Sol. State Comm. 27, 1029 (1978).

19. R.D. Dupuis and P.D. Dapkus, Appl. Phys. Lett. 33, 724 (1978).

20. N. Holonyak, Jr., R.M. Kolbas, W.D. Laidig, B.A. Vojak, R.D. Dupuis and P.D. Dapkus, Appl. Phys. Lett. 49, 5392 (1978).

21. N. Holonyak, Jr., R.M. Kolbas, E.A. Resek, R. Chin, R.D. Dupuis and P.D. Dapkus, Appl. Phys. Lett. 49, 5392 (1978).

22. N. Holonyak, Jr., R.M. Kolbas, W.D. Laidig, B.A. Vojak, R.D. Dupuis and P.D. Dapkus, in "Gallium Arsenide and Related Compounds 1978," Inst. of Physics, London, 1979, pp. 387-395.

23. R.D. Dupuis, P.D. Dapkus, R. Chin, N. Holonyak, Jr. and S.W. Kirchoefer, Appl. Phys. Lett. 34, 265 (1979).

24. R.D. Dupuis and P.D. Dapkus, IEEE J. of Quantum Electron. QE-15, 128 (1979).

25. R.D. Dupuis, P.D. Dapkus, N. Holonyak, Jr., R.M. Kolbas, W.D. Laidig and B.A. Vojak, Pisma Zh. Teh. Fiz. 5, 132 (1979). [Sov. Tech. Phys. Lett. 5, to be published].

26. N. Holonyak, Jr., R.M. Kolbas, W.D. Laidig, M. Altarelli, R.D. Dupuis and P.D. Dapkus, Appl. Phys. Lett. 34, 501 (1979).

27. R.D. Dupuis, P.D. Dapkus, R.M. Kolbas and N. Holonyak, Jr., IEEE J. Quantum Electron. QE-15, to be published.

28. B.A. Vojak, S.W. Kirchoefer, N. Holonyak, Jr., R. Chin, R.D. Dupuis and P.D. Dapkus, J. Appl. Phys. 50, to be published.

29. B.A. Vojak, N. Holonyak, Jr., R. Chin, E.A. Rezek, R.D. Dupuis and P.D. Dapkus, Appl. Phys. Lett. 35, to be published.

30. R.A. Milano, T.H. Windhorn, E.R. Anderson, G.E. Stillman, R.D. Dupuis and P.D. Dapkus, Appl. Phys. Lett. 34, 562 (1979).

31. R.E. Nahory, M.A. Pullock, E.D. Beebe and J.C. DeWinter, Appl. Phys. Lett. 27, 356 (1975).

32. R. Chin and C.M. Hill, Appl. Phys. Lett. 40, 332 (1982).

33. M.F. Gratton, R.G. Goodchild, L.Y. Juravel and J.C. Woolley, Jr. Electron. Mat. 8, 25 (1979).

APPENDIX I
DIRECT-INDIRECT TRANSITION IN GaAlAsSb

For optical-electronic devices, especially light sources, an issue of immense importance is the efficiency of the conversion of electrical energy to optical energy. It is well-known that the efficiency (electrical to optical energy) of a light emitter depends critically on whether the material is direct or indirect. If it is indirect, e.g., silicon, the material is an extremely poor light emitter. At the other extreme, materials such as GaAs or InGaAsP, which are direct, have extremely high efficiencies and can act as laser sources. Depending on the ratio of GaAs (direct) to GaP (indirect), $GaAs_{1-y}P_x$ can be fabricated which can be direct or indirect. Its efficiency can, therefore, range from extremely high to extremely low. It is known that beyond $y \sim 0.3$ the efficiency declines rapidly until the direct-indirect transition ($y \sim 0.44$) is reached. At this point, the material becomes indirect and is no longer useful as an efficienct light emitter.

The same issue is of importance in the GaAlAsSb system. Both GaSb and GaAs are both direct materials, and AlSb and AlAs are indirect materials. The exact nature of the direct-indirect transition is not known for the GaAlAsSb alloy system. However, theoretical approximations can be made from the ternary boundary conditions. The calculations take into account the relative population of electrons in the direct and indirect minima to determine the luminescence efficiency of the material. The results of such calculations are shown in Fig. A for GaAlAsSb lattice-matched to GaSb, InAs and InP. Since various assumptions were made in the calculation, these plots serve to indicate what may be expected.

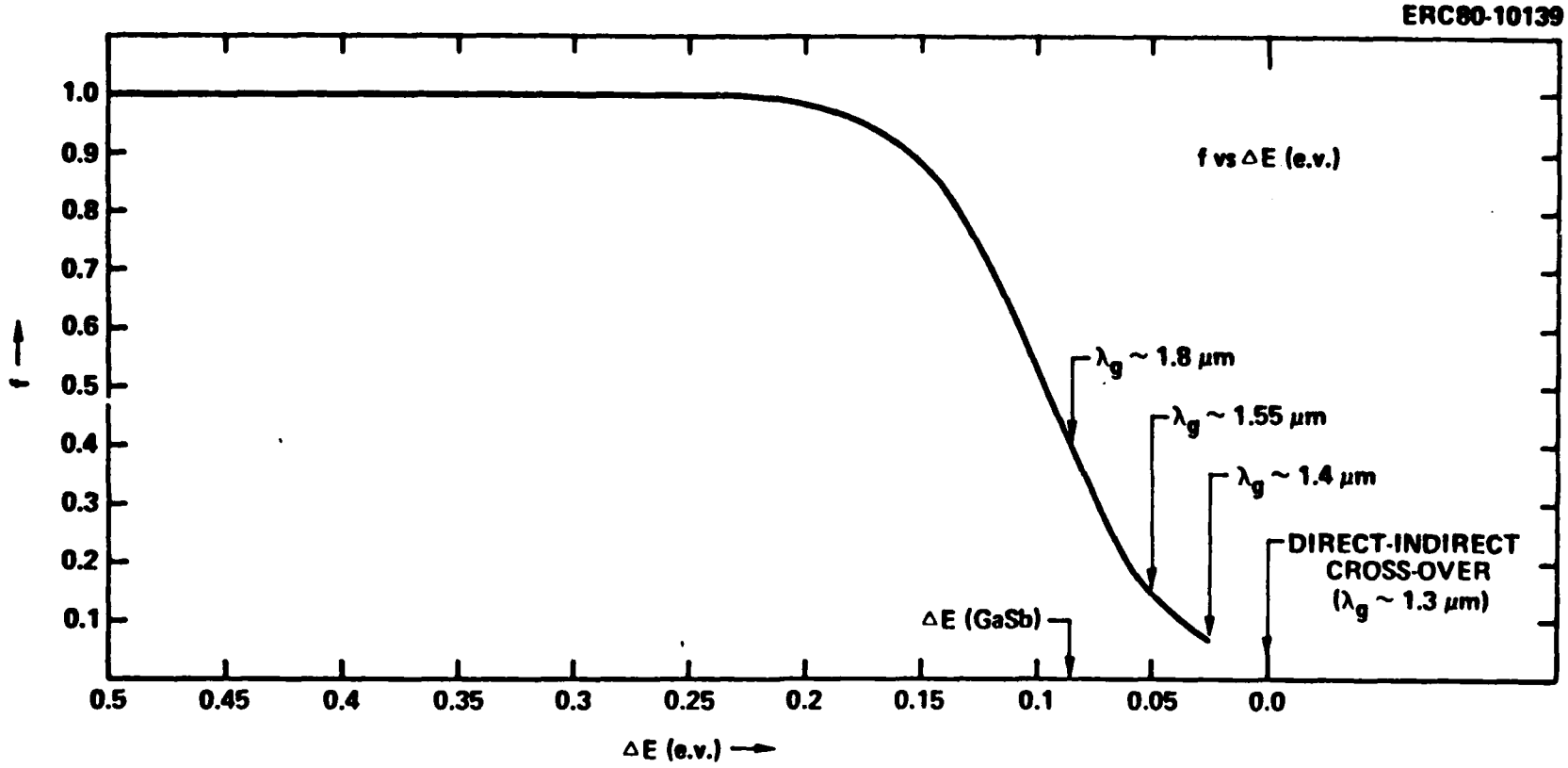

Fig. A Fraction f of electrons in the direct conduction band as a function of the separation between the direct and indirect conduction band minima.

APPENDIX II
REACTOR DESIGN AND GROWTH PROCEDURE

The basic CVD reactor design affects, to some degree, the pregrowth gas flow procedure. However, the general procedure used here is the procedure employed on previous reactors. A photograph of the CVD reactor is shown in Fig. B. Although the reactor is described in great detail in the first quarterly report, a brief description is given here. The hydride gases enter the reactor via a series of traps and pressure regulators. Mass flow controllers are utilized to control the rate of gas flow. When the gases are needed in the reactor, they are injected into the main gas stream through the use of air operated valves. The metalorganic complexes also enter the reactor in a similar manner. Purified H_2 gas flows through a series of traps to remove water-vapor and through the mass flow controllers. The H_2 gas is then bubbled through passivated 316-stainless steel bubblers holding the metalorganics. These are seen in the center of Fig. B. The metalorganic-bearing gas is then injected into the main gas stream when needed. The main gas stream flows into the reactor vessel where pyrolysis occurs and deposition takes place. The temperature of the susceptor is monitored with an optical pyrometer.

Following the loading of the substrate into the susceptor, the susceptor, which is attached to a motor-driven rotation platform, is allowed to rotate. During this time, the susceptor is empirically aligned to be centered. This aids in reducing nonuniform gas flow conditions. A quartz envelope is lowered onto an O-ring seat and the envelope is clamped tight. The chamber is sealed at both ends through a series of valves and then evacuated. The chamber is pumped to a pressure level of 1 μm. Hydrogen gas is then allowed to backfill the growth chamber via the gas handling apparatus until the pressure is slightly above atmospheric pressure. At this time, the exit valve is rotated open. The gas is allowed to purge the growth chamber for 15 minutes and then heating is commenced. The susceptor is rf heated to a temperature in the range from 450°C to 600°C. Usually, stabilization of the temperature necessary for epitaxial growth is less than 20 minutes. After the

MRDC81-14615

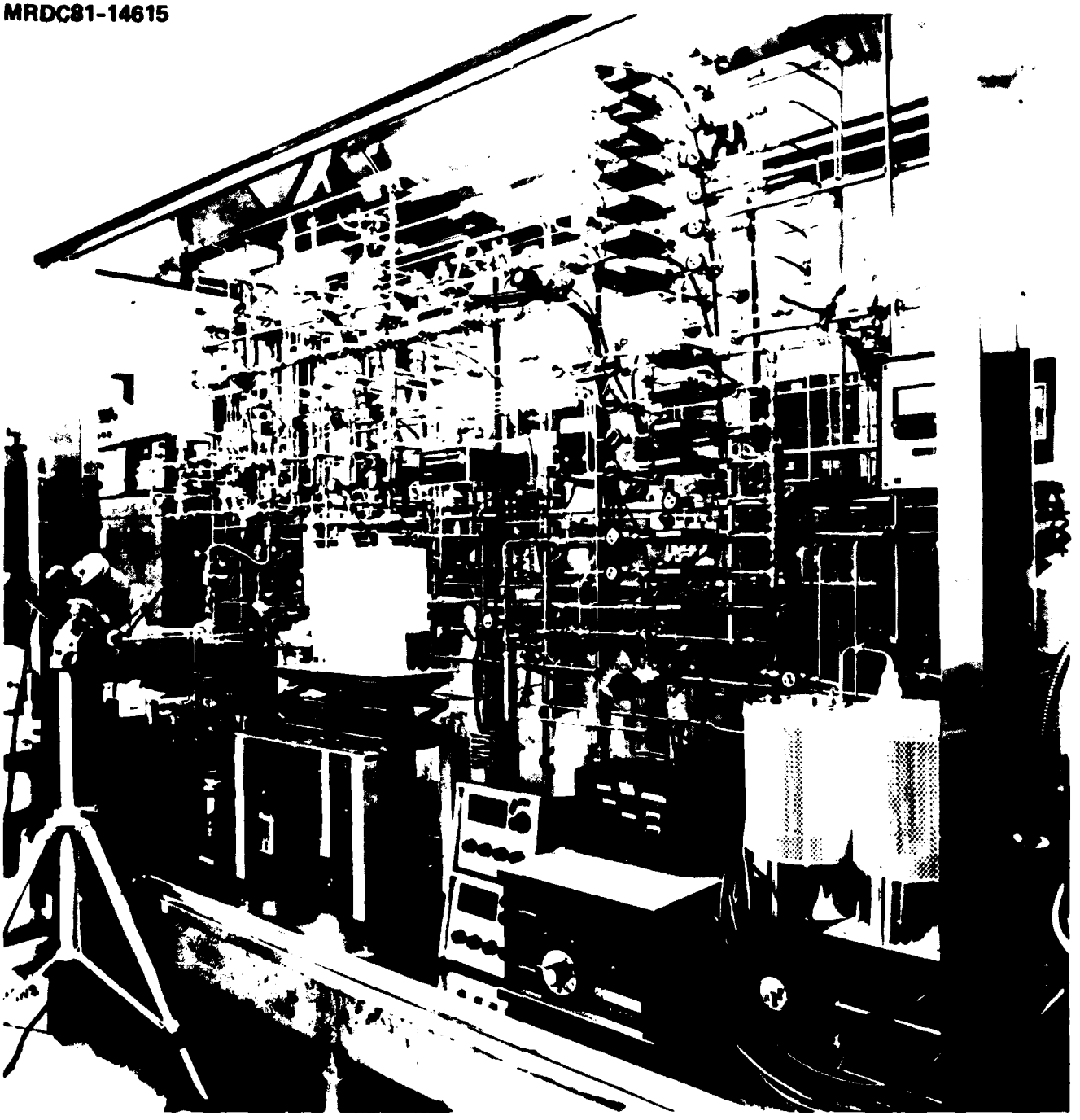

Fig. B Front view photograph of the MOCVD reactor used for the growth of GaAlAsSb.

temperature of the susceptor becomes stable (±1°C), the H_2 gas bubbled through the metalorganics is injected into the main H_2 gas (purge) stream. The resulting mixture flows over the heated susceptor; pyrolysis of the metalorganics occurs and epitaxial crystal growth commences.

When the epitaxial growth process is completed, the H_2 gas flow which bubbles through the metalorganics is shut off, and power to the rf generator power is also turned off. A H_2 cover gas is allowed to flow over the susceptor until the reactor cools to near ambient temperature. This process takes approximately 15 minutes. All gas flows are then stopped and the wafers removed for characterization. The susceptor, as well as some support apparatus, is cleaned and made ready for the next experiment.

APPENDIX III

THERMODYNAMIC PROPERTIES OF TEG AND TMG

A brief summary of the thermodynamic properties of TEGa and TMGa as they apply to the growth to epitaxial films is presented. Following the summary are two tables, one of which provides the conversion between the ratio of the flow rates of the metalorganics to the molar ratio of the alkyls.

The four major thermodynamic properties are now discussed. First, the molar heat of vaporization of $(CH_3CH_2)_3Ga$ is ~ 1.3 times that of $(CH_3)_3Ga$. The effect of this is that TEGa requires more expenditure of heat to effect equilibrium between the liquid and the gas phase than is required for TMGa. Second, the higher molar heat of vaporization of TEGa compared to TMGa, together with the low vapor pressure characteristics of TEGa, necessitates the use of high H_2 flow rates through the TEGa bubbler for longer periods of time in order to achieve useful film thicknesses. These requirements make growth rate and thickness control more difficult. For TEGa/TMSb molar injection ratios from 188/1 to 226/1 and growth temperatures between 550°C and 600°C, the growth rate of GaSb was only approximately 250Å/min. Third, the free energy of vaporization of TEGa is ~ 2.3 times greater than that of TMGa. Finally, the equilibrium constant for vapor-liqud equilibrium of TMGa is ~ 14.3 times that of TEGa. Hence, the density of TMGa molecules available for reaction will be much greater than the number of TEGa molecules.

AD-A133 123 ALGAASSB VAPOR PHASE EPITAXY AND LASER PROGRAM(U) 2/2
ROCKWELL INTERNATIONAL THOUSAND OAKS CA
MICROELECTRONICS RESE... R CHIN JUN 83 MRDC41078.9FR
UNCLASSIFIED RADC-TR-83-127 F19628-80-C-0130 F/G 20/12 NL

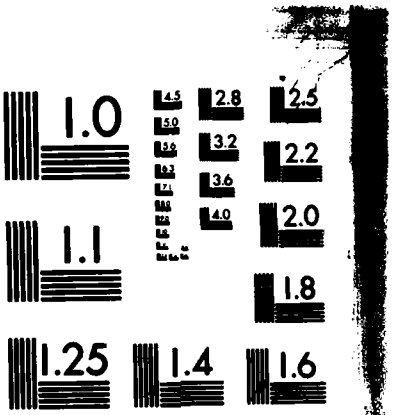

Table 1

Comparison of Thermodynamic Properties of TEGa and TMGa

Thermodynamic Property[a]	TEGa	TMGa
• Molar heat of vaporization, $\overline{\Delta H_v}$, kcal mole^{-1}	9.9	7.8
• Vapor pressure of R_3M at T°C	4.5 mm @ 18°C	64 mm @ 0°C
• Free energy of vaporization, ΔF_v, kcal mole^{-1}	3.0	1.3
• Metal alkyl liquid-gas equilibrium constant	5.9×10^{-3}	3.4×10^{-2}

a. Calculations of these thermodynamic properties of R_3M based upon the Gibbs-Helmholtz relation for chemical equilibrium at constant pressure and any given temperature:

$$\frac{\partial(\Delta F/T)}{\partial T}_P = -\frac{OH}{T^2}$$

Table 2

Summary of TEGa/TMSb Molar Injection Ratios

R_3M	Flow (cppm @ T°C)	Saturated Moles[a]	TEGa/TMSb (Molar Ratio)
TEGa	250 @ 18°	4.75×10^{-3}	349/1
TMSb	7 @ 0°	1.36×10^{-5}	
TEGa	250 @ 18°	4.75×10^{-3}	188/1
TMSb	13 @ 0°	2.52×10^{-5}	
TEGa	250 @ 18°	4.75×10^{-3}	49/1
TMSb	50 @ 0°	9.68×10^{-5}	
TEGa	300 @ 18°	5.70×10^{-3}	226/1
TMSb	13 @ 0°	2.52×10^{-5}	
TEGa	320 @ 18°	6.08×10^{-3}	125/1
TMSb	25 @ 0°	4.84×10^{-5}	
TEGa	495 @ 18°	9.50×10^{-3}	98/1
TMSb	50 @ 0°	9.08×10^{-5}	

a. Calculated for R_3M compounds from

$$n_i = \frac{[e^{2303(A-BT)^{-1}}](\text{flow rate } H_2)}{RT}$$

where A and B are constants characteristic of each metal alkyl.

APPENDIX IV

AsH_3 REQUIREMENTS FOR LATTICE-MATCHED GaAsSb-InAs

Calculation of amount of AsH_3/H_2 for growth of $GaAs_xSb_{1-x}$ alloy material, $x \approx 0.10$.

Vapor pressure equation for $(CH_3)_3Sb$:

$$\log P - 7.7280 - 1709\ T^{-1}$$

at 273K, $P_{TMSb} = 29.4$ Torr.

The saturated # moles of TMSb exiting the bubbler per unit time, n_{Sb}, is calculated as follows:

$$n_{Sb} = PV/RT$$

where

P = saturated equilibrium vapor pressure of TMSb at 273K
V = flow rate of H_2 through bubbler
R = gas constant
T = equilibrium temperature of bubbler

For V = 100 ccpm at T = 237K, $n_{Sb} = 17.05 \times 10^{-5}$mole.

If 10% (x = 0.10) of the Sb sites are to be occupied by As atoms, then to a first approximation

$$N_{As} = 0.10\ n_{Sb}$$
$$= 17.05 \times 10^{-6}\text{moles As.}$$

If each mole of As originates from a mole of arsine, then the number of moles of arsine required will be 17.05×10^{-6}. Initial growth experiments

use 10% AsH_3/H_2. Hence, for a AsH_3/H_2 flow rate of 4 ccpm, there will be approximately 0.4 ccpm of AsH_3 entering the growth chamber.

$$\frac{1 \text{ mole } AsH_3}{22{,}400 \text{ cc}} = \frac{x \text{ mole } AsH_3}{0.4 \text{ cc}}$$

$$x \approx 17.86 \times 10^{-6} \text{ mole}$$

To a first approximation, ~ 4 ccpm of 10% AsH_3/H_2 will be required to grow $GaAs_{0.10}Sb_{0.90}$ layers.

MISSION
of
Rome Air Development Center

RADC plans and executes research, development, test and selected acquisition programs in support of Command, Control Communications and Intelligence (C^3I) activities. Technical and engineering support within areas of technical competence is provided to ESD Program Offices (POs) and other ESD elements. The principal technical mission areas are communications, electromagnetic guidance and control, surveillance of ground and aerospace objects, intelligence data collection and handling, information system technology, ionospheric propagation, solid state sciences, microwave physics and electronic reliability, maintainability and compatibility.

Printed by
United States Air Force
Hanscom AFB, Mass. 01731


FILM